WASP FAMILY MEMBERS AND THE ARP2/3 COMPLEX ARE CRITICAL REGULATORS OF ACTIN IN THE DEVELOPMENT OF DENDRITIC SPINES AND SYNAPSES IN HIPPOCAMPAL NEURONS

By

Adam Michael Wegner

Dissertation

Submitted to the Faculty of the

Graduate School of Vanderbilt University

in partial fulfillment of the requirements

for the degree of

DOCTOR OF PHILOSOPHY

in

Neuroscience

May, 2008

Nashville, Tennessee

Approved:

Professor Terry L. Page

Professor Donna J.Webb

Professor Alissa M. Weaver

Professor Gregory C. Mathews

ACKNOWLEDGEMENTS

First and foremost I would like to thank my mom and dad for always being there for me and supporting me in whatever I have chosen to do. I would also like to thank Mary for her understanding as I spent many long hours at the lab working on experiments and writing. I am grateful for my weekly lunches with Stacy Johnson; I would not have been able to keep my sanity during the toughest moments of graduate school if it she hadn't been there to listen. Emmanuel Botzolakis also provided many ours of scientific and personal discussions which helped me immensely along the way.

I would like to thank the Interdisciplinary Program in the Biological Science for bringing me to Vanderbilt and the Neuroscience Graduate Program and Elaine Sanders-Bush for taking me in. I owe a great debt of gratitude to the program and Elaine for supporting me with the Neuroscience Training Grant and, along with Lou DeFelice, aiding me in my decision to switch labs.

I greatly appreciate the contributions of my dissertation committee of Terry Page, Greg Mathews, and Alissa Weaver for working with me in my unique situation and providing exceptional guidance and ideas en route to publishing a paper and defending in a limited time frame.

I would like to thank Donna Webb for accepting the challenge of having a 6th year graduate student transfer into her lab and try to graduate in a timely manner. She has been extremely supportive and instrumental in helping me regain my confidence as a scientist. The Webb lab has been an amazing place to work, and I am especially grateful for the assistance of Caroline Nebhan who helped quantify a majority of the experiments

presented here, Lan Hu for her expertise in molecular biology and the neuronal culture prep, and Devi Majumdar and Kristen Meier for their assistance with several experiments. Thank you to the rest of the Webb lab for constructive comments during lab meetings and making the lab an enjoyable place to spend time. This work was also made possible through funding from the National Institute of Mental Health.

Finally, I would like to thank Brian Wadzinski and the entire Wadzinski lab for helping to shape me as a person and scientist and teach me how to critically analyze data and design effective experiments. I also appreciate the thoughts and comments from the Colbran lab during our often lengthy joint lab meetings during my first several years of graduate school.

TABLE OF CONTENTS

Page

ACKNOWLEDGEMENTS ii

LIST OF FIGURES vi

LIST OF ABBREVIATIONS viii

Chapter

I. INTRODUCTION 1

Dendritic spine formation 2
WASP Family of Proteins 2
Wiskott-Aldrich Syndrome and the discovery of WASP family proteins 2
Domain Structure of WASP family proteins 5
N-WASP 8
N-WASP in cell biology 8
N-WASP in neurite extension 10
Other N-WASP functions in the nervous system 13
WAVEs 14
WAVEs in the CNS 14
WAVEs in dendritic spine formation 16
Cdc42 18
Cdc42 activation of N-WASP 18
Cdc42 in dendritic spine morphogenesis 19
The Arp2/3 Complex 19
The Arp2/3 complex in neurons 22
Summary and hypothesis 22

II. MATERIALS AND METHODS 24

Cell Culture and transfection 24
Immunohistochemistry 27
Image acquisition and analysis 28
Western blot analysis 29

III. N-WASP AND THE ARP2/3 COMPLEX REGULATE THE DEVELOPMENT OF DENDRITIC SPINES AND SYNAPSES 30

Introduction 30

Experimental Procedures 31
Reagents 31
Plasmids 32
Cell Culture and transfection 32
Immunohistochemistry and image analysis 33
FM4-64 loading and destaining 33
Results 34
N-WASP is enriched in excitatory synapses in hippocampal neurons 34
N-WASP regulates dendritic spine morphology and the formation of excitatory synapses 39
The actin and Arp2/3 binding domains of N-WASP are critical for its function in regulating spine and synapse formation 48
Cdc42 plays a role in the development of dendritic spines and synapses 52
Arp3 regulates the formation of spines and synapses in hippocampal neurons 55
Discussion 58

IV. WAVE1 IN SPINE AND SYNAPSE FORMATION 63

Introduction 63
Experimental Procedures 64
Reagents 64
Plasmids 64
Results 64
Discussion 65

V. CONCLUSIONS AND FUTURE DIRECTIONS 70

Future directions 71

Appendix

A. DETAILED SYNAPSE COUNTING PROTOCOL 74

B. “COUNT NUCLEI” MODULE INSTRUCTIONS 78

REFERENCES 82

LIST OF FIGURES

Figure		Page
1.	Dendritic Spine Development	3
2.	N-WASP	6
3.	Initiation of actin polymerization by the Arp2/3 complex and a WCA domain	20
4.	Rat hippocampal culture protocol	25
5.	Calcium phosphate neuron transfection with EGFP	26
6.	Endogenous N-WASP localizes to spines and synapses in hippocampal neurons	35
7.	GFP-N-WASP localizes to spines and synapses in hippocampal neurons	37
8.	N-WASP localizes to a majority of synapses in hippocampal neurons	38
9.	N-WASP localizes to functional synapses in hippocampal neurons	40
10.	Inhibition of N-WASP activity by Wiskostatin decreases spines and synapses	42
11.	Inhibition of N-WASP activity by Wiskostatin has no effect on inhibitory synapses	43
12.	Inhibition of N-WASP activity by Wiskostatin decreases excitatory synapses	44
13.	Specific knockdown of N-WASP in HEK-293 cells	46
14.	Knockdown of endogenous N-WASP affects spines and synapses in hippocampal neurons	47
15.	Domain Structure of N-WASP	50
16.	N-WASP binding to actin and the Arp2/3 complex is important for dendritic spine and synapse formation	51

17. Knockdown of endogenous Cdc42 in Rat2 fibroblasts.....53

18. Cdc42 plays a role in the development of dendritic spines and synapses 54

19. Endogenous and Gfp-Arp3 localize to spines and synapses in hippocampal neurons 56

20. Knockdown of Arp3 in HEK-293 cells 57

21. The Arp2/3 complex regulates the formation of dendritic spines and synapses in hippocampal neurons.....58

22. WAVE1 binding to actin and the Arp2/3 complex is important for dendritic spine and synapse formation.....67

23. Knockdown of WAVE1 in HEK-293 cells.....68

24. Knockdown of endogenous WAVE1 affects spines and synapses in hippocampal neurons 69

LIST OF ABBREVIATIONS

A	Acidic Domain
Abp1	Mammalian F-actin binding protein
Arp	Actin related protein
Ash	Abundant Src homology
B	Basic region
BAR	Bin–amphiphysin–rvs
BSA	Bovine serum albumen
Cdc42	Cell division cycle 42
C	Cofilin homology domain
CCD	Charge-coupled device
Cdk5	Cyclin dependent kinase 5
CNS	Central nervous system
CRMP-2	Collapsin response mediator protein 2
CR-16	Corticosteroids and regional expression-16
CRIB	Cdc42/Rac interactive binding domain
D	Aspartic acid
DCC	Deleted in colorectal cancer
DMEM	Dulbecco’s modified Eagle’s media
DNA	Deoxyribonucleic acid
EGFP	Enhanced GFP
EVH1	Ena/VASP homology 1

F-actin	Filamentous actin
G-actin	Monomeric actin
GBD	GTPase binding domain
GAD	Glutamic acid decarboxylase
GEFs	Guanine nucleotide exchange factors
GFP	Green fluorescent protein
Grb2	Growth factor receptor-bound protein 2
GTP	Guanosine triphosphate
HBS	HEPES buffered saline
HBSS	Hank’s buffered salt solution
HEK	Human embryonic kidney
HSP90	Heat shock protein 90
IQ	Calmodulin binding domain
IRSp53	Insulin receptor substrate p53
kDa	Kilodalton
mDAB1	Mouse disabled homolog 1
MEM	Modified essential media
NPF	Nucleation promoting factor
N-WASP	Neural Wiskott-Aldrich syndrome protein
PAK	p21 associated kinase
PBS	Phosphate buffered saline
PFA	Paraformaldehyde
PH	Pleckstrin homology domain

PIP_2	Phosphatidylinositol 4,5-bisphosphate
PIP_3	Phosphatidylinositol (3,4,5)-trisphosphate
PSD-95	Postsynaptic density-95
polyPro	Polyproline domain
RNA	Ribonucleic acid
Scar	Suppressor of the cAMP receptor
SDS	Sodium dodecyl sulfate
SDS-PAGE	SDS-polyacrylamide gel electrophoresis
SEM	Standard error of the mean
SH3	Src homology 3
SNX9	Sorting nexin 9
Src	Sarcoma
SV	Synaptic vesicle
RNAi	Ribonucleic acid interference
TBST	Triton-containing Tris-buffered saline
Toca-1	Transducer of Cdc42 dependent actin assembly
TRITC	Tetramethyl rhodamine isothiocyanate
V	Verprolin homology domain
VASP	Vasodilator-stimulated phosphoprotein
VCA	Verprolin, cofilin, and acidic domain
WA	WH2 and A domain
WAS	Wiskott-Aldrich syndrome
WASP	WAS protein

WAVE	WASP verprolin homologous protein
WICH/WIRE	WIP- and CR16-homologous protein/WIP-related
WIP	WASP interacting protein
WH1	WASP homology 1 domain
WH2	WASP homology 2 domain
WRP	WAVE-associated Rac GTPase activating protein

CHAPTER I

INTRODUCTION

Communication between neurons occurs at highly specialized cell-cell junctions called synapses. These structures are composed of a pre- and post-synaptic terminal that allow for propagation of signals between neurons and are the basis for the complex circuitry found in the central nervous system (CNS). Postsynaptic terminals of excitatory synapses consist of actin-rich dendritic spines (Matus et al., 1982), which are small extensions from the dendrite that form connections with axonal terminals. The small post synaptic compartments created by the spine are hypothesized to form a biochemically unique microenvironment suited to the function and regulation of the particular synapse. Abnormalities in dendritic spines are associated with various neurological and psychiatric disorders, including mental retardation, schizophrenia, epilepsy, and Alzheimer's disease, pointing to the importance of these structures in the CNS (Fiala et al., 2002). Morphological changes in dendritic spines due to reorganization of the actin cytoskeleton are thought to be important for synaptic function, and thus, integrating information flow within the brain (Dunaevsky et al., 1999; Fischer et al., 1998; Harris, 1999; Matus, 2000). Despite considerable interest, the molecular mechanisms that regulate spine morphology and synapse formation via modulation of the actin cytoskeleton are poorly understood.

Dendritic Spine Formation

At some point, formation of a dendritic spine must involve protrusion from the dendrite toward the presynaptic terminal, and the driving force behind this motility is thought be actin polymerization (Matus, 2000). One theory of spine morphogenesis states that a spine originates as a highly motile short lived (10 min) filopodia that extends up to 10 μm from the dendritic shaft (Figure 1) (Portera-Cailliau et al., 2003; Ziv and Smith, 1996). The factors which direct these filopodia toward the presynaptic site of an axon are unclear; however, once in contact with a suitable presynaptic partner, the filopodia begin to stabilize and form adhesions to the presynaptic site (Washbourne et al., 2004). Dendritic spines contain more filamentous actin (F-actin) than filopodia (Calabrese et al., 2006), so maturation from filopodia to dendritic spine must also require regulated actin polymerization. Although the actual structure of the underlying actin skeleton of dendritic spines is unknown, enlargement of the spine head, which is necessary for the formation of mature mushroom shaped dendritic spines, likely requires the formation of branched actin structures.

WASP Family of Proteins

Wiskott-Aldrich Syndrome and the discovery of WASP family proteins

Wiskott-Aldrich syndrome (WAS) is an X-linked genetic disease characterized by an increased tendency to bleed due to low platelet counts, eczema of the skin, and recurrent infections due to immunodeficiency involving both B and T lymphocytes (Ochs and Thrasher, 2006). The gene responsible for this disease, Wiskott-Aldrich syndrome

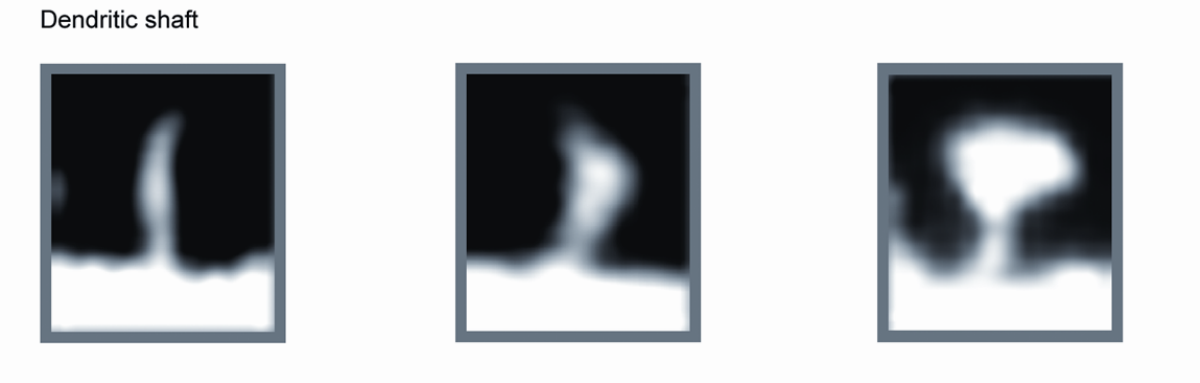

Figure 1. Dendritic spine development

Rhodamine-phalloidin stained cultured hippocampal neurons demonstrating development of a dendritic spine and that spines are rich in actin. One model of spine morphogenesis involves initial protrusion (left), stabilization of the protrusion (middle), and maturation into a mushroom shaped dendritic spine (right).

protein (WASP), was cloned by Derry et al. (1994), who used positional cloning to identify the gene on the X-chromosome responsible for the disease. They also identified 3 different mutations in exon 2 of WASP in three unrelated patients, confirming that mutations of this gene cause the disease. Its expression was restricted to hematopoietic cells of lymphocytes, spleen, and thymus, and defects in these cells correlate with the symptoms of WAS described earlier. WASP was discovered to be involved in the regulation of actin polymerization (Symons et al., 1996), and this explained the abnormal cell architecture, trafficking, and migration of hematopoietic cells from WAS patients (Ochs and Thrasher, 2006).

Several years after the discovery of WASP, a 65 kDa protein with 50% homology to WASP was discovered in a screen for abundant sarcoma (Src) homology/growth factor receptor-bound protein 2 (Ash/Grb2) interacting proteins from bovine brain (Miki et al., 1996). Although this novel protein was expressed ubiquitously in brain, lung, heart and colon, it was most abundant in the brain, resulting in the name neural WASP (N-WASP). This novel protein bound actin and depolymerized actin *in vitro*, and overexpression in COS-7 cells affected actin polymerization (Miki et al., 1996). The human homolog of N-WASP was subsequently cloned by the same group and found to be expressed throughout the brain (Fukuoka et al., 1997).

Three other members of the WASP family of proteins have been identified to date, and all contain a similar domain arrangement as WASP and N-WASP. WASP family verprolin homologous protein 1 (WAVE1) was identified through a database search for proteins containing sequences similar to the highly conserved verprolin homology domains of WASP and N-WASP. It was only expressed in the brain (Nagase et al.,

1996), and was found to be a regulator of actin polymerization downstream of Rac (Miki et al., 1998b). Further database and library screening identified WAVE2, which was expressed ubiquitously except for skeletal muscle, and WAVE3, whose expression was restricted to the brain (Suetsugu et al., 1999).

Domain Structure of WASP family proteins

The VCA region of WASP family proteins, consisting of the verprolin homology domain (V), cofilin homology domain (C, also known as the central domain), and acidic domain (A), is at the extreme C-terminus of all WASP family proteins (Figure 2). The V domain, also known as a WASP homology 2 (WH2) domain (for review see Paunola et al. (2002)), directly binds monomeric actin (G-actin) (Chereau et al., 2005). In the case of N-WASP, it was originally thought to cooperate with the C domain to sever actin filaments (Miki and Takenawa, 1998), but is now thought to deliver the first actin monomer to initiate polymerization of a new actin filament (Goley and Welch, 2006) The C and A domains bind the Arp2/3 complex, and, along with the V domain, activate Arp2/3 nucleation of new actin branches at a fixed 70° angle to the original filament (Amann and Pollard, 2001; Mullins et al., 1998; Rohatgi et al., 1999). N-WASP is unique among WASP family members in that it contains two consecutive V domains, and this feature allows for more potent stimulation of actin polymerization than the VCA regions of the other family members which contain only one V domain (Yamaguchi et al., 2000). Adjacent to the VCA regions of all WASP family proteins is a proline rich region, the polyPro domain, which is important for binding of profilin (Suetsugu et al., 1998) and Src homology 3 (SH3) domain containing proteins (Takenawa and Suetsugu, 2007) by

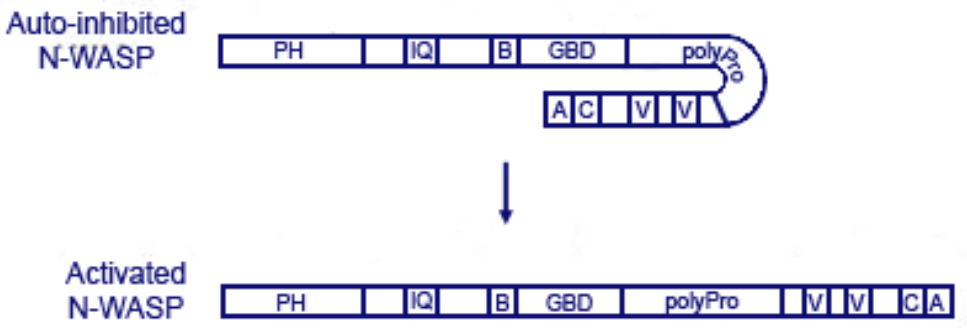

Figure 2. N-WASP

Free N-WASP favors the auto-inhibited conformation, top. Binding of Cdc42 to the GBD domain and PIP_2 to the B domain shifts the equilibrium to the active conformation, bottom. Domains: Pleckstrin homology (PH), calmodulin binding (IQ), basic (B), GTPase binding domain (GBD), poly-proline domain (polyPro), verprolin homology (V), central (C), and acidic (A). Modified from (Stamm et al., 2005).

WASP, N-WASP, and WAVE1, and insulin receptor substrate p53 (IRSp53) by WAVE2 (Miki et al., 2000).

Although the C-terminal regions of WASP family members are similar, the N termini contain unique domains allowing for activation by diverse upstream signals. WASP and N-WASP, but not the WAVEs, contain an N-terminal WASP homology 1 (WH1) domain, also called an Ena-VASP homology domain (EVH1). WASP interacting protein (WIP) (Ramesh et al., 1997), corticosteroids and regional expression-16 (CR-16) (Ho et al., 2001), and WIP- and CR16-homologous protein/WIP-related (WICH/WIRE) (Aspenstrom, 2002; Kato et al., 2002) all form complexes with the WASP and N-WASP WH1 domains and regulate activation of actin polymerization (for review see Anton and Jones (2006)). The WH1 domain of WASP and N-WASP, which was originally identified as a pleckstrin homology (PH) domain, also cooperates with an adjacent basic (B) region to bind phosphatidylinositol 4,5-bisphosphate (PIP_2) (Miki et al., 1996), an interaction which has been shown to be involved in the activation of actin polymerization by WASP and N-WASP (Prehoda et al., 2000). The extreme N-termini of the WAVEs consist of a WAVE homology domain/Suppressor of the cAMP receptor (Scar) homology domain (WHD/SHD). The WAVE2 WHD/SHD binds Phosphatidylinositol (3,4,5)-trisphosphate (PIP_3) in cooperation with the basic region, which is important in the formation of lamellipodia (Oikawa et al., 2004).

WASP and N-WASP, but not the WAVEs, have a Cdc42/Rac interactive binding (CRIB) domain, sometimes called the GTPase binding (GBD) domain, C-terminal to the WH1 and basic region. Cdc42 binds to the CRIB/GBD domain and activates WASP (Symons et al., 1996) and N-WASP (Miki et al., 1998a). Other small GTPases such as

Tc10, RhoT, and Chp also bind and activate N-WASP (Abe et al., 2003; Aronheim et al., 1998).

At rest, WASP and N-WASP exist in an autoinhibited conformation (Figure 2), where the C-terminal VCA region folds back onto the CRIB/GBD and other surrounding regions (Miki et al., 1998a; Rohatgi et al., 1999). This predicted conformation was visualized by a crystal structure which showed that WASP VCA binds to the CRIB/GBD and induces formation of a compact, folded domain immediately C-terminal (Kim et al., 2000). There is no autoinhibition within WAVE proteins because they do not posses a CRIB/GBD. Instead, they integrate into pentameric heterocomplexes called WAVE complexes, which keep them inactive until upstream signals release them (Eden et al., 2002; Innocenti et al., 2004; Stovold et al., 2005; Suetsugu et al., 2006).

N-WASP

N-WASP in cell biology

N-WASP plays a wide variety of roles in processes requiring regulation of actin polymerization, such as cell motility and pathogen infection, as well as the process of transcription. N-WASP is most well known and characterized for its role in actin based cell motility in non-neuronal cells. N-WASP has been implicated in the formation of filopodia and invadopodia. During the initial discovery of N-WASP, it was observed that overexpression of N-WASP in COS-7 cells, along with EGF stimulation, caused the formation of microspikes (Miki et al., 1996). The same group later showed that Cdc42 activation of N-WASP caused extension of filopodia in COS-7 cells and Swiss 3T3

fibroblasts (Miki et al., 1998a), but it was shown shortly thereafter that N-WASP is not required for all filopodial protrusions (Snapper et al., 2001). N-WASP knockout mice were generated, and although they did not survive past embryonic day12, 50% of cells derived from the embryos were still able to form normal lamellipodia and filopodia when injected with active Cdc42. This indicates that N-WASP is not necessary for the formation of all Cdc42 induced filopodia. This is not surprising, since it is counterintuitive to think that N-WASP initiates filopodia formation. Filopodia contain bundled actin filaments (Lewis and Bridgman, 1992), while N-WASP induced actin polymerization produces branched filaments (Blanchoin et al., 2000; Pantaloni et al., 2000).

Other functions of N-WASP activation of the Arp2/3 complex include regulation of podosome formation in macrophages and invadopodium formation in certain types of cancer cells (Linder and Aepfelbacher, 2003; Sturge et al., 2002; Yamaguchi et al., 2005). Recently, it was reported that N-WASP is involved in dorsal ruffle formation in mouse embryonic fibroblasts as well as migration in ovarian tumor cells (Bourguignon et al., 2007; Legg et al., 2007). N-WASP has also been shown to be involved in regulating actin polymerization during vesicular trafficking, and, specifically, endocytosis through syndapin I and Bin–amphiphysin–rvs (BAR) domain containing proteins (Itoh et al., 2005; Qualmann and Kelly, 2000).

N-WASP in the nucleus plays a role in regulating polymerization of nuclear actin for RNA-polymerase-II dependent transcription through binding to a large nuclear protein complex (Wu et al., 2006). It has also been reported that nuclear localization of N-WASP is regulated by tyrosine phosphorylation, and when in the nucleus, it binds heat

shock transcription factor to regulate heat shock protein 90 (HSP90) expression (Suetsugu and Takenawa, 2003). A role for N-WASP in pathogen infection has been shown for actin based motility of *Shigella flexneri* (Suzuki et al., 1998) and vaccinia virus (Frischknecht et al., 1999), actin pedestal formation of *Escherichia coli* (Lommel et al., 2001), internalization of *Yersinia pseudotuberculosis* (McGee et al., 2001), and actin tail formation of *Mycobacterium marinum* (Stamm et al., 2005).

N-WASP in neurite extension

The most well studied role for N-WASP in the nervous system is its influence on neurite extension in the developing neuron. Several cell types, including PC-12, N1E-155, and primary rat hippocampal neurons have been used to study this phenomenon. A majority of reports have shown that N-WASP activity is required for extension of neurites, although there is some conflicting evidence that N-WASP activity inhibits neurite extension.

An N-WASP that did not efficiently activate Arp2/3 complex was generated by mutating 4 residues in the cofilin homology domain (Δcof) corresponding to mutations found in the WASP of a subset of WAS patients. When Δcof or the N-WASP H208D mutant, which is unable to bind Cdc42, was expressed in PC-12 cells, NGF and cAMP were not able to stimulate normal neurite outgrowth. Interestingly, the double Δcof-H208D mutant failed to suppress outgrowth, suggesting that Cdc42 was able to signal to the Arp2/3 complex through endogenous N-WASP and the individual mutants acted as dominant negatives. Infection of primary rat hippocampal cultures with the Δcof mutant also inhibited neurite outgrowth (Banzai et al., 2000).

N-WASP was found to be involved in neurite extension in PC-12 and N1E-115 cells downstream of Tc10 and a related novel Rho GTPase, RhoT, and this effect was blocked by the dominant negative H208D mutant of N-WASP (Abe et al., 2003). Interestingly, constitutively active Cdc42, despite the fact that it binds to the N-WASP CRIB domain like Tc10 and RhoT, did not induce neuritogenesis in these cells.

Suetsugu et al. (2002) further elaborated on this mechanism in PC12 cells, N1E-115 cells, and primary hippocampal neurons, showing sustained activation of N-WASP through phosphorylation by Fyn, a Src family kinase. The N-WASP Y253F mutation eliminating the necessary tyrosine phosphorylation site significantly reduced neurite outgrowth in primary hippocampal neurons.

Suetsugu et al. (2002) also found that phosphorylation of N-WASP during proliferative conditions, rather than conditions favoring neurite outgrowth, resulted in ubiquitination and degradation of N-WASP. Park et al. (2005) further investigated the degradation of N-WASP, and found that HSP90 regulates N-WASP induced actin polymerization along with tyrosine phosphorylation. HSP90 does not regulate Arp2/3 complex activation by N-WASP; rather, it protects phosphorylated N-WASP from proteasomal degradation, which helps sustain the N-WASP mediated initiation of actin polymerization, and as a result, is a positive regulator of neurite extension.

Two N-WASP interacting proteins, the novel protein Rapostlin (Kakimoto et al., 2004) and the recently discovered transducer of Cdc42 dependent actin assembly (Toca-1) (Ho et al., 2004), were found to regulate N-WASP in neurite extension. Rapostlin was shown to bind N-WASP through its SH3 domain and regulate neurite branching downstream of Rnd2, a novel Rho family GTPase, in PC-12 cells (Kakimoto et al.,

2004). Toca-1 initiated formation of a complex by binding N-WASP and Cdc42 through its SH3 and HR1 domains, respectively. Knockdown of either N-WASP or Toca-1 in PC-12 cells increased neurite elongation. This data is in direct conflict with previous data using dominant negative N-WASP, which showed that expression of N-WASP H208D in PC12 cells decreased neurite extension (Banzai et al., 2000). Knockdown of N-WASP in cultured rat hippocampal neurons enhanced axon elongation and branching, while knockdown of Toca-1 only enhanced branching (Kakimoto et al., 2006).

N-WASP has been shown to have a role in netrin-1 induced axon growth cone expansion in cultured primary neurons. Netrin-1 is a protein that guides migrating cells and axons, and its function in cultured hippocampal neurons requires Cdc42, Rac1, p21 activated kinase 1 (PAK1), and N-WASP (Shekarabi et al., 2005). Application of netrin-1 rapidly induced Cdc42, Rac1, and PAK1 activity as well as formation of a complex with Cdc42, Rac1, PAK1 and N-WASP with the intracellular domain of deleted in colorectal cancer (DCC) and Nck1.

Recently, the mammalian F-actin binding protein (Abp1), was shown to directly interact with N-WASP through its SH3 domain and activate it along with Cdc42 to control neurite extension (Pinyol et al., 2007). N-WASP, Arp2/3, and Abp1 colocalize at sites of actin polymerization in growth cones and throughout the dendritic arbors of cultured hippocampal neurons that were hypothesized to be sites of synaptic contact. Knockdown of N-WASP, Abp1, and Arp2/3, as well as expression of N-WASP lacking the proline rich domain (Abp1 binding), all resulted in increased axon length.

Finally, a recent study in PC-12 cells demonstrated an antagonistic role for Cdc42 and Tc10 in control of N-WASP activity in neurite extension. Knockdown of N-WASP

and expression of dominant negative N-WASP-Δcof or H208D implicated N-WASP in Exo70/Tc10 mediated NGF induced membrane protrusion (Pommereit and Wouters, 2007). Use of a FRET biosensor showed that Exo70 and constitutively active Tc10 antagonized NGF induced Cdc42 dependent N-WASP activity.

Other N-WASP functions in the nervous system

N-WASP has been implicated in other neuronal and non-neuronal processes requiring regulation of actin polymerization in the nervous system, including neural progenitor migration, synaptic vesicle trafficking, oligodendrocyte formation, along with preliminary evidence that it is involved in the formation of dendritic spines (Irie and Yamaguchi, 2002).

Mouse disabled homolog 1 (mDab1) is a protein directly downstream of Reelin, which is a key molecule in determining cell position in the developing nervous system. It has been shown that mDab1 directly binds to N-WASP and induces actin polymerization through the Arp2/3 complex (Suetsugu et al., 2004).

The protein sorting nexin 9 (SNX9) has been linked to clathrin mediated endocytosis, and recently has been found in the presynaptic compartment in cultured hippocampal neurons (Shin et al., 2007). SNX9 binds to dynamin and N-WASP through its SH3 domain, and mutation in the domain that eliminates N-WASP binding decreases endocytosis.

N-WASP also appears to be important for the formation of oligodendrocytes and the production of myelin. Inhibition of N-WASP by the specific inhibitor wiskostatin blocks process extension by oligodendrocyte precursor cells and Schwann cells, and

application of the inhibitor after extension causes rapid retraction (Bacon et al., 2007). Wiskostatin treatment also decreases the number of axons undergoing myelination in optic nerve samples and decreases expression of the glycoprotein Po in dorsal root ganglion:Schwann cell co-cultures, indicating decreased myelination.

Most important for this study, several groups have preliminary data implicating N-WASP in synapse formation and dendritic spine dynamics. A hallmark of Alzheimer's disease is abnormal neuronal sprouting of spike-like filopodial structures and growth cone like lamellipodia (McKee et al., 1989). These structures are the result of aberrant regulation of actin polymerization, but the mechanism of their formation is still not well understood. In order to investigate the role of WASP family proteins as potential causes of this phenotype, Kitamura et al. (2003) obtained tissue samples from postmortem brains of patients suffering from Alzheimer's disease and showed significant increases in levels of N-WASP, WAVE, and WISH compared to normal brains. N-WASP has also been implicated in synaptic growth in *Aplysia* sensory neurons. Dominant negative Cdc42 or the CRIB domain of N-WASP reduced long term changes in synaptic structure induced by serotonin mediated plasticity (Udo et al., 2005).

WAVEs

WAVEs in the CNS

Studies in *Drosophila* showed that fly orthologs of Scar/WAVE1 complex components are found in developing axons. Knockdown of several members of the complex all result in similar phenotypes including aberrant axonal migration and a

decrease in synapses (Schenck et al., 2004). The similarity of the phenotypes may be explained by decreased expression of all members of the complex when expression of one component is decreased.

The mechanism by which the WAVE1 complex localizes to axons was studied by Kawano et al. (2005). The collapsin response mediator protein 2 (CRMP-2) was found to associate with the Sra-1/WAVE1 complex and regulate axonal growth. RNAi mediated knockdown of WAVE1 abolished CRMP-2 mediated axon outgrowth and multiple-axon formation, leading to the hypothesis that CRMP-2 transports the Sra-1/WAVE1 complex into axons where it regulates axon outgrowth and formation.

A WAVE1 knockout mouse was generated to evaluate its role in development of the nervous system. The knockout had an average lifespan of 23 days and exhibited severe limb weakness, resting tremors. Their brains had gross neuroanatomical defects, but no changes in neuronal morphology were observed (Dahl et al., 2003). Cultured cortical neurons from E15 mice were normal at 5 days in culture when assessed for neurite length and number. This indicated that WAVE1 was important for neural development, but not necessary for extension of neurites. WAVE1 did appear to be involved in oligodendrocyte morphogenesis and myelination. WAVE1 localized to the leading edge of lamellipodia of cultured oligodendrocytes, and expression of dominant negative WAVE1 decreased outgrowth (Kim et al., 2006a). Oligodendrocytes isolated from the WAVE1 knockout mice had fewer processes while astrocytes and neurons appeared normal. The knockout mice also exhibited reduced myelination in the corpus collosum and optic nerve (Kim et al., 2006a).

WAVEs in dendritic spine formation

There is evidence for all 3 WAVE proteins in various aspects of spine morphogenesis or plasticity. To this point, the role of the WAVE proteins in the formation and plasticity of dendritic spines is more defined than that of N-WASP. GFP-WAVE3 was shown to localize to spines in a manner not requiring the C-terminal VCA domains (Pilpel and Segal, 2005). Overexpression of full length GFP-WAVE3 decreased spine density, and this effect was mediated by the VCA domain, as expression of GFP-WAVE3-ΔVCA had no effect on spines. Also, spinogenesis stimulated by glutamate caused translocation of WAVE3 into the tip of newly formed dendritic spines (Pilpel and Segal, 2005). There is also one report implicating WAVE2 in spine morphogenesis (Choi et al., 2005). IRSp53, whose SH3 domain has been shown to bind the polyPro domain of WAVE2 (Miki et al., 2000), links Cdc42/Rac1 signals to downstream actin regulators in non-neuronal cells (Govind et al., 2001; Krugmann et al., 2001). The density and size of spines was decreased when IRSp53 with a point mutation in the SH3 domain or WAVE2 with a dominant negative polyPro region was expressed.

Very recently, several papers have connected WAVE1 with the development and plasticity of dendritic spines. Cultured medium spiny neurons from the WAVE1 knockout mouse and cultured hippocampal neurons at 8 days in culture transfected with a WAVE1 RNAi construct showed a decrease in spine density (Kim et al., 2006b). This report also implicated the phosphorylation of WAVE1 in spine formation. Transfection of the WAVE1 RNAi construct along with an RNAi resistant WAVE1 S310D, a mutant to mimic phosphorylation at a cyclin dependent kinase 5 (Cdk5) site, into cultured

hippocampal neurons resulted in an increase in filopodia and a decrease in mature dendritic spines.

WAVE1 has been shown to localize to synapses, as cultured hippocampal neurons from wild-type mice at 21 days in culture immunostained for WAVE1 and postsynaptic density 95 (PSD-95) showed colocalization (Soderling et al., 2007). Also, a 20% decease in the number dendritic spines in Golgi impregnated hippocampal slices from the WAVE1 knockout mouse was seen when compared to slices from wild-type controls. Electrophysiological analysis of hippocampal slices from the knockout mice showed changes in synaptic input-output ratio, train induced LTP, and paired pulse induced LTD compared to wild-type controls. These changes in spine density and electrophysiological responses were found to be dependent on WAVE1 binding to WAVE-associated Rac GTPase activating protein (WRP) (Soderling et al., 2007). Generation of a transgenic mouse expressing WAVE1 lacking WRP binding sites showed similar phenotypes to those seen in the WAVE1 knockout. Finally, behavioral analysis found that disruption of WRP binding to WAVE1 decreases performance in the Morris water maze (Soderling et al., 2007), indicating learning and memory defects.

WAVE1 has also been linked to mitochondrial trafficking to dendritic protrusions. Mitochondria have been implicated in the formation of dendritic spines, in that they provide a local source of ATP for spine morphogenesis (Li et al., 2004). When cultured hippocampal neurons were transfected with a mitochondrial marker, stimulated with repeated K+ depolarizations, and stained for WAVE1, a significant colocalization of WAVE1 and mitochondria was observed (Sung et al., 2008). Also, RNAi mediated

knockdown of WAVE1 reduces mitochondrial trafficking to spines, and this function of WAVE1 was also tied to its phosphorylation by Cdk5 (Sung et al., 2008).

Cdc42

Cdc42 is a member of the Rho family of small GTPases. GTPases are small guanine nucleotide binding proteins which exist in two forms: active-GTP bound and inactive-GDP bound. When bound to GTP, Rho family GTPases signal to downstream effectors controlling the actin cytoskeleton, providing the driving force for changes in cell morphology and migration. Changes in Rho GTPase signaling have been linked to changes in neuron morphology and mental retardation (Govek et al., 2005; Newey et al., 2005).

Cdc42 activation of N-WASP

Through a yeast two-hybrid screen, Cdc42 was initially discovered to bind WASP through the region now known as the CRIB/GBD (Aspenstrom et al., 1996), and subsequently, WASP was shown to be a downstream effector of Cdc42, but not Rac or Rho (Symons et al., 1996). N-WASP was implicated as an effector of Cdc42 when it was shown that N-WASP, but not WASP, enhanced filopodium formation induced by Cdc42 (Miki et al., 1998a). Binding of PIP_2 to the basic region of N-WASP, just C-terminal to the CRIB/GBD, cooperates with Cdc42 binding to maximally activate N-WASP (Higgs and Pollard, 2000; Papayannopoulos et al., 2005; Prehoda et al., 2000; Rohatgi et al., 2000). Grb2 binding has also been shown to cooperate with Cdc42 to activate N-WASP through binding of its SH3 domain to the polyPro region of N-WASP (Carlier et al.,

2000). Phosphorylation of the CRIB/GBD by the Src family tyrosine kinase may also act in concert with Cdc42 to active N-WASP (Torres and Rosen, 2006).

Cdc42 in dendritic spine morphogenesis

There are conflicting reports on the role of Cdc42 in the formation of dendritic spines. Several studies using constitutively active (Cdc42-HsV17) and dominant negative (Cdc42-N17) Cdc42 in cultured hippocampal neurons or organotypic slices have shown no effect on spine density or length (Govek et al., 2004; Tashiro et al., 2000). However, other studies suggest otherwise. Manipulation of several Cdc42 guanine nucleotide exchange factors (GEFs), including ARHGEF6, intersectin, GEFT, and βPIX have been shown to affect dendritic spine density (Bryan et al., 2004; Irie and Yamaguchi, 2002; Nishimura et al., 2006; Node-Langlois et al., 2006; Park et al., 2003). Expression of a loss-of-function Cdc42 in *Drosophila* vertical system neurons showed a 50% decrease in dendritic spines (Scott et al., 2003), and Cdc42 was also shown to play a role in learning related synaptic growth in *Aplysia (Udo et al., 2005)*. Manipulation of IRSp53, a downstream effector of Rac1/Cdc42, in cultured hippocampal neurons caused changes in dendritic spine formation and morphology (Choi et al., 2005). Finally, a recent report using cultured hippocampal neurons and organotypic slices linked a Cdc42/PAK3 module to dendritic spine formation (Kreis et al., 2007).

The Arp2/3 Complex

Actin provides a mechanical support for cells and the driving force for cell movement and cytokinesis. The generation of branched actin filaments catalyzed by the

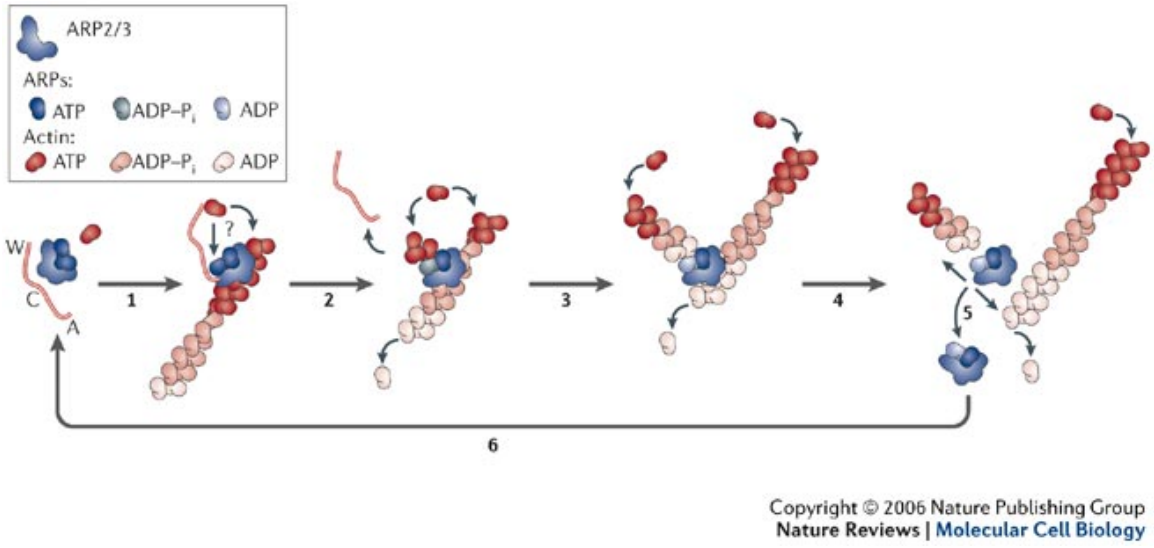

Figure 3. Initiation of actin polymerization by the Arp2/3 complex and a WCA domain.

Nucleation of actin polymerization from an existing filament by the Arp2/3 complex and a WCA (WASP homology 2 (also known as verprolin homology(V)), central/cofilin homology (C), acidic (A)) region from a WASP family member. Reprinted from Goley et al. (2006).

Arp2/3 complex is important for generation of this support network (Pollard, 2007). By anchoring the pointed end of a new actin filament to an existing filament, the Arp2/3 nucleates new filaments at a fixed 70° angle, with the free barbed end able to extend until polymerization is terminated by a capping protein (Figure 3) (Amann and Pollard, 2001; Blanchoin et al., 2000; Mullins et al., 1998; Pantaloni et al., 2000). The 7 member Arp2/3 complex is composed of two actin-related proteins, Arp2 and Arp3, and 5 other novel subunits, ARPC1-5 (Machesky et al., 1994; Welch et al., 1997a).

The Arp2/3 complex exists in an inactive state until activated by a nucleation promoting factor (NPF). All members of the WASP family are NPFs, and are able to perform this function by binding and activating the Arp2/3 complex (Machesky and Insall, 1998; Machesky et al., 1999; Yarar et al., 1999). Isolated full length N-WASP is not an efficient activator of the Arp2/3 complex, but the N-WASP VCA region by itself is 100 times more potent at stimulating Arp2/3 mediated actin polymerization (Rohatgi et al., 1999). Cdc42 was known to activate Arp2/3 mediated actin polymerization (Ma et al., 1998), and this provided the missing link in the activation of Arp2/3 by N-WASP. It was found that Cdc42, along with PIP_2, could fully activate full length N-WASP mediated actin polymerization by the Arp2/3 complex to the same extent as the N-WASP VCA fragment alone (Higgs and Pollard, 2000; Rohatgi et al., 1999), suggesting that Cdc42 was able to relieve the intramolecular inhibition within the resting state of N-WASP that prevented its ability to activate the Arp2/3 complex.

The interaction of the Arp2/3 complex with N-WASP has been narrowed down to the C and A domains (Marchand et al., 2001; Panchal et al., 2003), but the entire VCA region is required for full activation of actin polymerization by the complex (Hufner et

al., 2001). N-WASP has two V domains, while the other WASP family members only have 1, and these two V domains allow N-WASP to be a more potent activator of Arp2/3 mediated actin polymerization than the other family members (Yamaguchi et al., 2000; Yamaguchi et al., 2002; Zalevsky et al., 2001). This leads to a model of actin polymerization where the CA region binds to Arp2/3 and the V domains bind actin monomers which can be used to initiate the new actin filament (Figure 3). Recently, a more subtle model was proposed where the C domain first binds to Arp2/3 to prime the complex, then binds an actin monomer to initiate filament assembly (Goley et al., 2004; Kelly et al., 2006; Rodal et al., 2005).

The Arp2/3 complex in neurons

Since the Arp2/3 complex is the only known actin effector downstream of all WASP family proteins, it has the potential to be involved in all of the neuronal processes implicating N-WASP and WAVEs, as well as other NPFs known to activate the complex. The Arp2/3 complex has been specifically implicated in neurite branching by several reports (Banzai et al., 2000; Kakimoto et al., 2006; Pinyol et al., 2007). It has also recently been shown to play a critical role in the generation of branched actin filaments for growth cone motility and neurite formation in cultured neurons (Goldberg et al., 2000; Korobova and Svitkina, 2008; Mongiu et al., 2007; Strasser et al., 2004).

Summary and Hypothesis

WASP family members regulate actin polymerization through binding and activation of the Arp2/3 complex in a wide variety of processes in neuronal and non-

neuronal cells. One important process that requires coordinated actin polymerization is the development and maturation of actin rich dendritic spines, which form the postsynaptic side of excitatory synapses in the central nervous system. However, the mechanisms which regulate the polymerization of actin in this process are poorly understood. We hypothesized that the WASP family members N-WASP and WAVE1, acting through the Arp2/3 complex, are necessary for the development of dendritic spines and synapses in rat hippocampal neurons.

CHAPTER II

MATERIALS AND METHODS

Cell Culture and Transfection

Hippocampal low density cultures were prepared as previously described (Figure 4) (Goslin et al., 1998). Briefly, hippocampi were removed from E18 rat brains and dissociated with 0.25% trypsin in Hank's buffered salt solution (HBSS) at 37º C for 15 minutes. The mixture was then pipetted vigorously and cells added dropwise to a 60 cm plate containing 5 x 1.5 cm diameter glass coverslips coated with poly-L-lysine. Neurons were plated at a density of 70,000 cells/mm^2. After 2-4 hours at 37º C, the coverslips were transferred to a new 60 mm plate containing a bed of glia and N2 media supplemented with B27 (GIBCO, Grand Island, NY). The coverslips were placed neuron side down and suspended over the bed of glia with three paraffin "feet".

Glia were prepared from neonatal rat pups. Cerebral hemispheres were dissected out and meninges removed. Hemispheres were finely chopped with scissors and dissociated with 0.25% trypsin and 0.1% DNase in BSS at 37° C. The mixture was filtered through sterile nylon mesh (215 μm) and diluted with a mixture of MEM and 10% horse serum to inhibit trypsin. Cells were then centrifuged at 800-1000 rpm and resuspended in MEM with 10% horse serum. 250,000 Glia were plated per 60 mm dish.

Neurons were transfected by a modified calcium phosphate precipitation method (Figure 5) (Zhang et al., 2003). Briefly, 6-12 μg of plasmid DNA was added to 120 μl of 250 mM $CaCl_2$, then 120 μl of 2X HBS (274 mM NaCl, 9.5 mM KCl, 15 mM glucose, 42 mM HEPES, 1.4 mM Na_2HPO_4, pH 7.05-7.10) was added drop wise while the

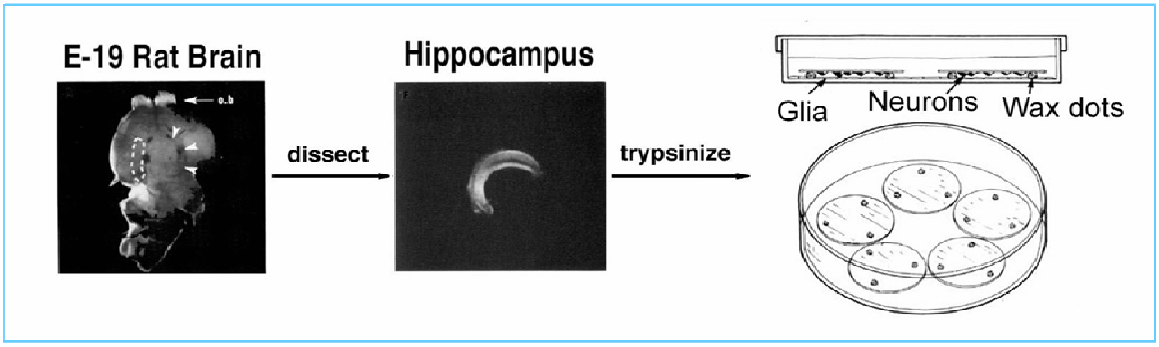

Figure 4. Rat hippocamal culture protocol

Hippocampi from E19 rat brains were dissociated with trypsin and plated on coverslips suspended over a bed of glia using the 'sandwich culture" method (right panel). Reprinted from Goslin et al. (1998).

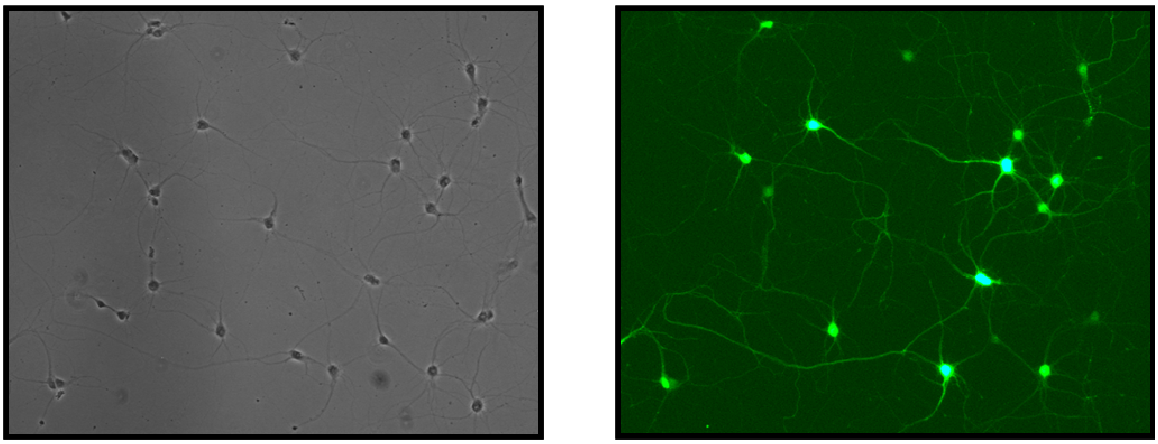

Figure 5. Calcium phosphate neuron transfection with EGFP

10 X Phase image (left) and fluorescence image (right) of cultured hippocampal neurons transfected with EGFP

mixture was aerated. The mixture was then immediately added drop wise to a 60 mm dish containing coverslips with the neuron side up, 2 ml GIBCO B27 supplemented neurobasal medium (Invitrogen, Carlsbad, CA), 2 ml 24-hour glia-conditioned neurobasal medium, and 0.5 mM kynurenic acid. After 45-75 min. of complex formation, the cells were washed three times with HBS (20 mM HEPES, pH 7.35, 135 mM NaCl, 4 mM KCl, 2 mM $CaCl_2$, 1 mM $MgCl_2$, 10 mM glucose) at 37º C and returned to the home dish supplemented with 0.5 mM kynurenic acid.

HEK-293T cells and Rat2 Fibroblasts (ATCC, Manassas, VA) were cultured in DMEM (Invitrogen) supplemented with 10% fetal bovine serum (FBS) and penicillin/streptomycin. HEK cells were transfected with Lipofectamine 2000 (Invitrogen) according to manufacturer's instructions. One day before transfection, cells were plated at density of 30,000 cells/cm^2 in a 6 well plate. 10 μl of Lipofectamine 2000 was diluted in 250 μl of Opti-MEM I Reduced Serum Medium (GIBCO) and, in a separate tube, 4 μg of DNA was diluted in 250 μl of Opti-MEM I and each tube was incubated at room temperature for 5 minutes. The DNA and Lipofectamine 2000 mixtures were combined, gently mixed, and incubated for 20 minutes at room temperature. The mixture was added dropwise to the well and mixed gently. Cells were then incubated at 37º C in a humid incubator for 72 hours before lysis.

Immunohistochemistry

For most antibodies, neurons were fixed with 4% paraformaldehyde (PFA)/4% glucose in phosphate-buffered saline (PBS, 5 mM NaH_2PO_4, 15 mM $NaHPO_4$, 150 mM NaCl, pH 7.4) for 15 min. Coverslips were then permeabilized with 0.2 % Triton-X in

PBS for 5 min and washed 3 times with PBS. For PSD-95 staining, neurons were fixed for 3 min with 4% PFA solution and then permeabilized for 10 min in cold methanol at -20º C. Coverslips were then blocked for 1 hour with 20% goat serum in PBS. Antibodies were diluted in 5% goat serum in PBS to the indicated dilutions and incubated for 1 hour at room temperature, followed by 3 washes with PBS. Coverslips were mounted with Aqua Poly/Mount (Polysciences, Inc., Warrington, PA) and sealed with clear fingernail polish.

Image Acquisition and Analysis

Neurons were imaged with a Retiga EXi CCD camera (QImaging, Surrey, BC) attached to an Olympus IX71 inverted microscope (Melville, NY) with a 10X (Olympus, numerical aperture 0.30) or 60X objective (Olympus, numerical aperture 1.45). Image acquisition was controlled by MetaMorph software (Molecular Devices, Sunnyvale, CA) interfaced with a Lambda 10-2 automated controller (Sutter Instruments, Novato, CA). For EGFP and Alexa Fluor® 488, an Endow GFP Bandpass filter cube (excitation HQ470/40, emission HQ525/50, Q495LP dichroic mirror) (Chroma, Brattleboro, VT) was used. Rhodamine, Alexa Fluor® 555, and FM4-64 FX were imaged with a TRITC/Cy3 cube (excitation HQ545/30, emission HQ610/75, Q570LP dichroic mirror) (Chroma).

Images were counted in MetaMorph using the “Count Nuclei” application module (for a detailed protocol see Appendix A). Briefly, the dendrite of interest was circled and copied to a new window. The synapses were counted by the application based on adjustment of minimum and maximum widths and intensity over background and verified

by eye. The distance of the dendrite counted was determined by MetaMorph, while Microsoft Excel was used to calculate synapses per 100 microns.

Western Blot Analysis

Three days after transfection, HEK-293T cells were harvested in lysis buffer containing 25 mM Tris, pH 7.4, 0.5% NP-40, 100 mM NaCl, and protease inhibitor cocktail (1:100, Sigma, St. Louis, MO), and spun for 10 minutes at 15,000 xg. Samples were diluted in 5X Laemmli sample buffer (312.5 mM tris-base, 50% glycerol, 10% SDS, 0.035% bromophenol blue) and boiled at 95º C for 10 minutes. 50 μg of protein, as determined by BCA assay (Pierce, Rockford, IL), were run on a 10% SDS-PAGE gel in Laemmli running buffer (25 mM tris-base, 0.192 M glycine, 0.1% SDS, pH 8.3) at 150 V for 1 hour and transferred to a nitrocellulose membrane at 300 mV for 1 hour in transfer buffer (10% Methanol, 30 mM tris-base, 240 mM glycine). Transferred protein was visualized with Ponceau S stain and washed with TBST (0.05% Tween-20, 10 mM Tris-base, 150 mM NaCl), and membranes were blocked for 1 hour. with 0.5% BSA in TBST. Membranes were then probed with primary antibodies for 1 hour, washed 3 times with TBST, probed with secondary for 30 minutes, and washed 3 times with TBST. Blots were scanned with an Odyssey infrared imaging system (Li-COR, Lincoln, NE), and quantified with Odyssey 2.0 software. For quantification, a best fit box was drawn around each band with the background set to “Median, Top/Bottom”.

CHAPTER III

N-WASP AND THE ARP2/3 COMPLEX REGULATE THE DEVELOPMENT OF DENDRITIC SPINES AND SYNAPSES

Introduction

Members of the Wiskott-Aldrich syndrome protein family, including WASP, neural WASP, and WASP-family verprolin homologous proteins are emerging as critical regulators of the actin cytoskeleton. These proteins initiate the nucleation of new actin filaments through activation of the Arp2/3 complex (Machesky et al., 1999; Rohatgi et al., 1999). New filaments generated by the Arp2/3 complex are formed at fixed angles to the mother filament, creating a branched actin network that is commonly found in protrusive regions of cells (Bailly et al., 1999; Mullins et al., 1998). C-terminal sequences within N-WASP, consisting of a verprolin-like homology domain (V), a central domain (C), and an acidic region (A), mediate binding of G-actin and Arp2/3 complex to these proteins, which subsequently results in actin nucleation (Blanchoin et al., 2000; Machesky et al., 1999; Rohatgi et al., 1999; Yamaguchi et al., 2000).

N-WASP, as its name implies, is highly expressed in the brain, but its function in the nervous system is not well understood (Miki et al., 1996). In this study, we show a crucial function for N-WASP in the formation of dendritic spines and synapses in hippocampal neurons. This activity of N-WASP is dependent on its C-terminal binding and activation of the Arp2/3 complex. Inhibition of Arp2/3 binding to N-WASP resulted in a significant reduction in the density of spines and synapses. Decreased expression of an N-WASP activator, Cdc42, also caused a defect in the formation of spines and

synapses. Thus, our results point to a critical role for activated N-WASP and the Arp2/3 complex in the development of dendritic spines and synapses in the CNS.

Experimental Procedures

Reagents

Synaptic vesicle 2 (SV2) (1:250) and glutamic acid decarboxylase-6 (GAD-6) (1:250) monoclonal antibodies were from the Developmental Studies Hybridoma Bank (The University of Iowa, Iowa City, IA). PSD-95 monoclonal antibody was from Chemicon (Temecula, CA). GFP polyclonal antibody was from Invitrogen (Carlsbad, CA). β-Actin AC-15 monoclonal antibody, α-tubulin DM 1A monoclonal antibody, and phalloidin-TRITC were from Sigma (St. Louis, MO). N-WASP (1:50) polyclonal antibody was a generous gift from Marc Kirschner (Harvard, Boston, MA). Arp3 antibody (1:100) was previously described (Yarar et al., 1999). Cdc42 monoclonal antibody (B-8) was from Santa Cruz Biotechnology (Santa Cruz, CA). Alexa Fluor® 488 and 555 anti-mouse, Alexa Fluor® 488 and 555 anti-rabbit for immunohistochemistry, Alexa Fluor® 680 anti-rabbit for western blotting, and FM4-64 FX were from Molecular Probes (Eugene, OR). IRDye® 800 anti-mouse for western blotting was from Rockland Immunochemicals (Gilbertsville, PA). Wiskostatin was purchased from Calbiochem (San Diego, CA).

Plasmids

Small interfering RNA (RNAi) constructs were prepared by ligating annealed sense and antisense 64mer-oligonucleotides into pSUPER vector as previously described (Zhang and Macara, 2008). The RNAi oligos contained the following 19 nucleotide target sequences: N-WASP RNAi, 5'-GACGAGATGCTCCAAATGG-3'; Arp3 RNAi, 5'AGGTTTATGGAGCAAGTGA-3'; Cdc42 RNAi, 5'-GGGCAAGAGGATTATG-ACA-3'; and scrambled RNAi 5'-CAGTCGCGTTTGCGACTGG-3'. The scrambled RNAi target sequence, which had been previously described (Saito et al., 2007), was used as a control. Full-length GFP-N-WASP and GFP-N-WASP-ΔWA, -WA, and -ΔWH1 were generous gifts from Michael Way (Lincoln's Inn Fields Laboratories, London, UK). GFP tagged bovine N-WASP was a generous gift from John Condeelis (Albert Einstein, Bronx, NY). GFP-Arp3 has been previously described (Welch et al., 1997b). Myc-tagged WAVE1 was kindly provided by Hiroaki Miki and Tadaomi Takenawa (Univ. of Tokyo, Japan). Myc-tagged dominant negative Cdc42 (Cdc42-N17) was a generous gift from Alan Hall (Memorial Sloan-Kettering, New York, NY).

Cell Culture and Transfection

Hippocampal low density cultures were prepared as previously described (Goslin et al., 1998). Neurons were plated at a density of 70,000 cells/mm^2 and transfected by a modified calcium phosphate method (Zhang et al., 2003). HEK-293T cells (ATCC, Manassas, VA) were cultured in DMEM (Invitrogen, Carlsbad, CA), supplemented with 10% fetal bovine serum (FBS) and penicillin/streptomycin. HEK cells were transfected with Lipofectamine 2000 (Invitrogen) according to the manufacturer's instructions.

Immunohistochemistry and Image Analysis

For most antibodies, neurons were fixed with 4% PFA/4% glucose in phosphate-buffered saline (PBS) for 15 min. Coverslips were then permeabilized with 0.2% Triton X-100 for 5 min and washed 3 times with PBS. For PSD-95 staining, neurons were fixed for 3 min with PFA solution and then permeabilized for 10 min in cold methanol at -20º C. Coverslips were then blocked for 1 hour with 20% goat serum in PBS. Antibodies were diluted in 5% goat serum in PBS and incubated at the indicated dilutions for 1 h followed by 3 washes with PBS. Coverslips were mounted with Aqua Poly/Mount (Polysciences, Inc., Warrington, PA).

Neurons were imaged with a Retiga EXi CCD camera (QImaging, Surrey, BC) attached to an Olympus IX71 inverted microscope (Melville, NY) with a 60X objective (Olympus, numerical aperture 1.45). Image acquisition was controlled by MetaMorph software (Molecular Devices, Sunnyvale, CA) interfaced with a Lambda 10-2 automated controller (Sutter Instruments, Novato, CA). For EGFP and Alexa Fluor® 488, an Endow GFP Bandpass filter cube (excitation HQ470/40, emission HQ525/50, Q495LP dichroic mirror) (Chroma, Brattleboro, VT) was used. Rhodamine and Alexa Fluor® 555 were imaged with a TRITC/Cy3 cube (excitation HQ545/30, emission HQ610/75, Q570LP dichroic mirror).

FM4-64 Loading and Destaining

Day 12 neurons were incubated with 0.5 μM FM4-64 FX in high K+ solution containing 72 mM NaCl, 50 mM KCl, 1mM NaH_2PO_4, 26 mM $NaHCO_3$, 1.8 mM $CaCl_2$, 0.8 mM $MgSO_4$, 11 mM D-glucose and 20 mM HEPES, pH 7.35 for 3 min. Neurons

were then washed 3 times with calcium free solution, fixed with 4% PFA/4% glucose for 15 min, and visualized by fluorescence microscopy.

Results

N-WASP is Enriched in Excitatory Synapses in Hippocampal Neurons

The expression of N-WASP has been shown to increase dramatically in the rat hippocampus during the first several weeks after birth (Tsuchiya et al., 2006), a time when dendritic spines and synapses are developing. This led us to hypothesize that this molecule plays an important role in spine and synapse formation. To begin to test our hypothesis, we examined the subcellular localization of N-WASP in hippocampal neurons by immunostaining low density cultures with N-WASP antibody along with a pre- and a post-synaptic marker. Endogenous N-WASP accumulated in puncta along neuronal processes with the synaptic vesicle protein SV2, and the postsynaptic density protein PSD-95, a marker for excitatory glutamatergic synapses (Figure 6, arrows). Since it is difficult to determine from the lower magnification images whether N-WASP puncta were completely merged or were in close apposition to the synaptic markers, higher magnification images were generated. As shown in the higher magnification images, N-WASP puncta were in close apposition to the presynaptic marker, SV2, suggesting it was in postsynaptic terminals (Figure 6). Consistent with this, N-WASP puncta almost completely merged with the postsynaptic marker PSD-95 (Figure 6), indicating that N-WASP localizes to the postsynaptic side of excitatory synapses. Although most N-WASP localized to excitatory synapses, a fraction of N-WASP puncta was negative for

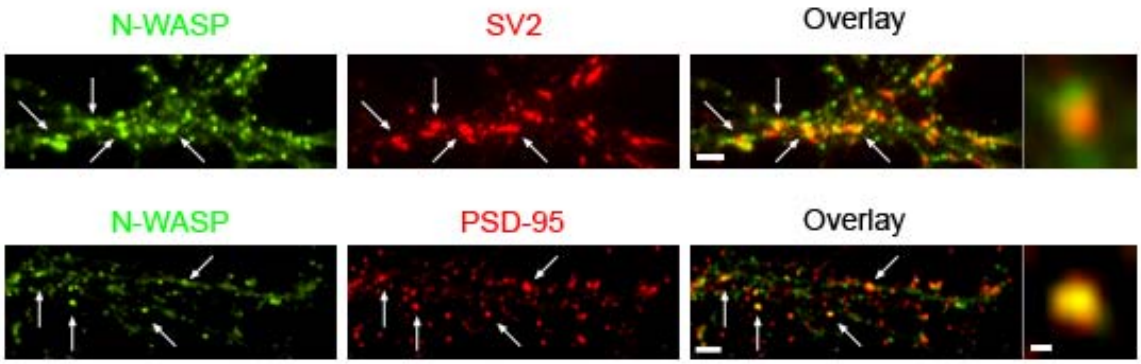

Figure 6. Endogenous N-WASP localizes to spines and synapses in hippocampal neurons.

Hippocampal neurons at day 12 in culture were co-immunostained for endogenous N-WASP and the presynaptic marker SV2 (upper panels) or the postsynaptic marker PSD-95 (lower panels). Endogenous N-WASP accumulated in puncta along neuronal processes with the synaptic markers (overlays, right panels, arrows). Bar = 2 μm. High magnification images showed that N-WASP puncta were in close apposition to SV2 and completely merged with PSD-95, indicating N-WASP is enriched in the postsynaptic side of excitatory synapses. Bar = 0.4 μm. PSD-95.

PSD-95. These puncta might represent N-WASP protein complexes that have been previously described in non-neuronal cells (Takenawa and Suetsugu, 2007).

The localization of N-WASP to synapses was confirmed by transfecting neurons with GFP-tagged N-WASP. The GFP tag was previously shown to have no effect on N-WASP localization (Moreau et al., 2000). Like endogenous N-WASP, GFP-N-WASP co-localized in clusters with PSD-95 and was in close apposition to SV2 clusters (Figure 7, arrows), confirming that N-WASP is enriched in the postsynaptic terminal of excitatory synapses. However, in both cases, some of the synapses lacked N-WASP, which led us to quantify the number of SV2 and PSD-95 synapses that contained N-WASP puncta. Approximately 55% of the SV2 clusters and about 66% of the PSD-95 clusters contained N-WASP (Figure 7), indicating that N-WASP is present in a majority of the excitatory synapses. Similar results were obtained with GFP-N-WASP. This raised the question as to whether the N-WASP containing synapses were activity-dependent, functional synapses.

FM4-64 is a member of a family of styryl dyes which can be used as fluorescent probes to visualize active synapses (Betz and Bewick, 1992; Betz et al., 1996). These dyes exhibit prominent fluorescence upon insertion of their hydrophobic tails into a lipid bilayer, but can easily be washed out due to their inability to cross bilayers (Cochilla et al., 1999). When a cell surface is exposed to an FM dye and then washed with a dye-free solution, only membranes that are no longer surface exposed retain the fluorescent dye (Cochilla et al., 1999). Thus, the activity-dependent uptake of FM dyes into synaptic vesicles provides a useful marker for functional synapses in cultured neurons (Betz et al., 1992; Ryan et al., 1993). To determine whether N-WASP containing synapses were

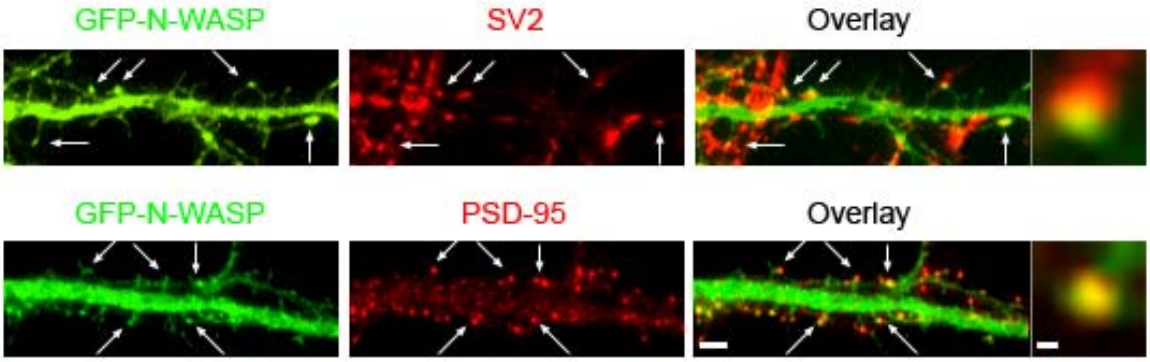

Figure 7. GFP-N-WASP localizes to spines and synapses in hippocampal neurons.

Hippocampal neurons were transfected with GFP-N-WASP at day 5 in culture and fixed and immunostained for SV2 (upper panels) and PSD-95 (lower panels) at day 12 culture. Like endogenous N-WASP, GFP-N-WASP localized in puncta with the synaptic markers SV2 and PSD-95, (arrows). Bar = 2 μm. High magnification images (right panels) showed that N-WASP puncta were in close apposition to SV2 and completely merged with PSD-95, indicating N-WASP is enriched in the postsynaptic terminal of excitatory synapses. Bar = 0.4 μm.

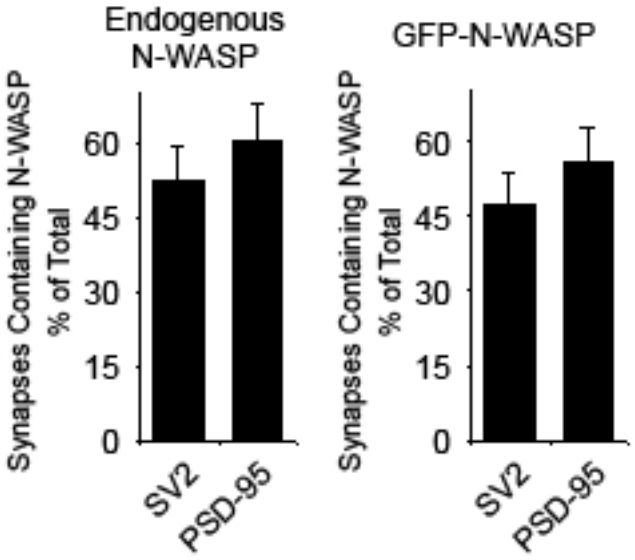

Figure 8. **N-WASP localizes to a majority of synapses in hippocampal neurons.**

Quantification of the percentage of SV2 and PSD-95 synapses that contain N-WASP.

functional, neurons expressing GFP-N-WASP were labeled with FM4-64. Day 12 neurons were incubated with 0.5 μM FM4-64 in high K+ solution for 3 minutes and then washed 3 times with calcium free solution. As expected, FM4-64 puncta, which represented functional synapses, was observed along the dendrites (Figure 9). However, when neurons were incubated with the dye in a buffer lacking K+, FM4-64 puncta were not observed, indicating that FM4-64 uptake is dependent on depolarization. As shown in Figure 9, N-WASP puncta localized with FM4-64. Quantification of these results showed that 85.0 ± 3.5% of the FM4-64 labeled synapses contained N-WASP, demonstrating that most of the active synapses had N-WASP. Thus, our results indicate N-WASP is present in the postsynaptic side of active, functional excitatory synapses that could undergo changes in morphology mediated by reorganization of the actin cytoskeleton.

N-WASP Regulates Dendritic Spine Morphology and the Formation of Excitatory Synapses

To examine the function of N-WASP in the neurons, we treated cultures with a specific inhibitor of N-WASP, wiskostatin, and determined the density of synapses and spines by staining with SV2 and phalloidin, respectively. Wiskostatin stabilizes the autoinhibited form of the protein so that the C-terminal VCA domains are not available to bind G-actin and the Arp2/3 complex to initiate new actin filaments (Peterson et al., 2004). When neurons were treated with wiskostatin at day 7, and fixed and immunostained at day 12, a dose dependent decrease in the number of spines and synapses was observed (Figure 10). Wiskostatin did not adversely affect the health of the neurons since they were observed to develop normally, and no detectable effects on the

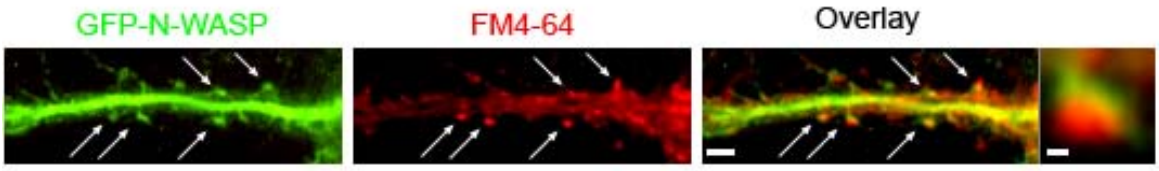

Figure 9. N-WASP localizes to functional synapses in hippocampal neurons.

Hippocampal neurons were transfected with GFP-N-WASP at day 5 in culture. At day 12 in culture, neurons were incubated with FM4-64 dye (0.5 μM) in high K+ solution for 3 minutes, washed, fixed, and viewed in fluorescence. FM4-64, which labels presynaptic terminals of active synapses, was in close apposition to N-WASP puncta (overlay, right panel, arrows, high magnification image), indicating that N-WASP containing synapses are functional. Bar = 2 μm. For the high magnification image, Bar = 0.4 μm.

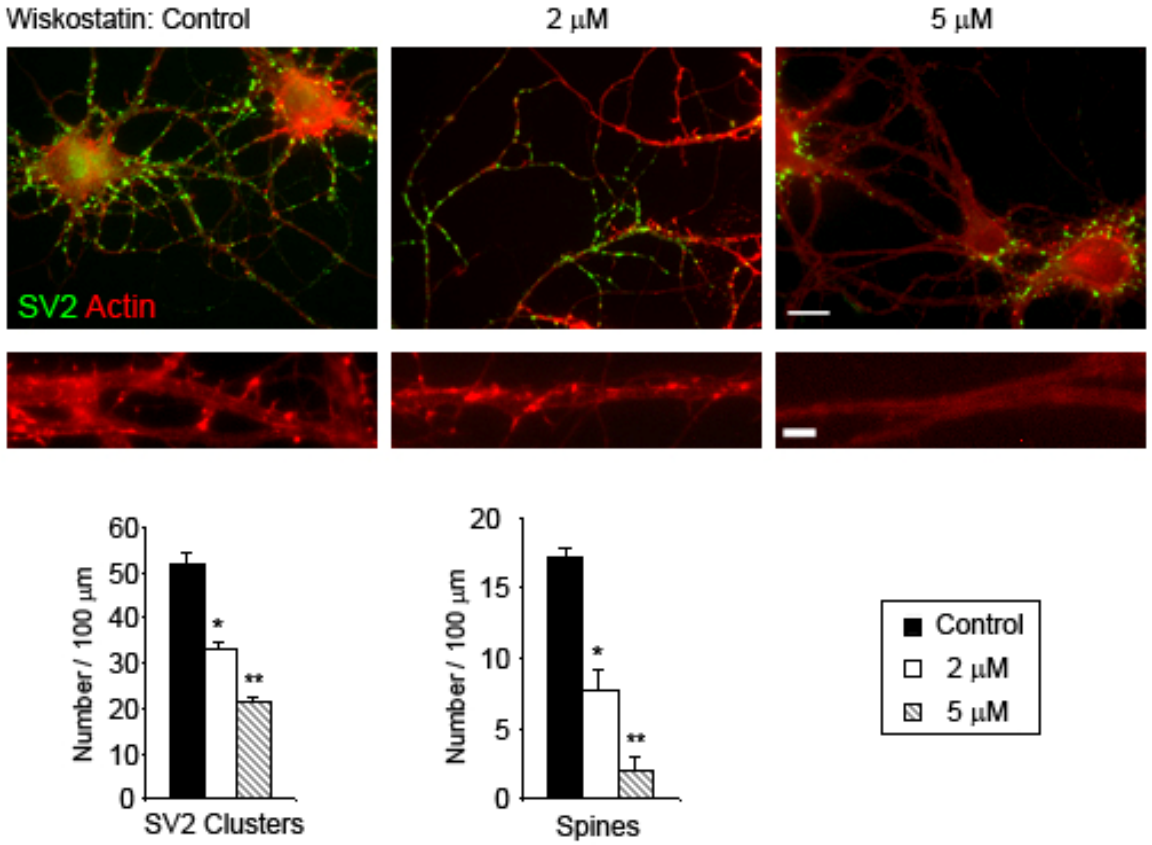

FIGURE 10. Inhibition of N-WASP activity by wiskostatin decreases spines and synapses.

Hippocampal neurons were treated with either DMSO (Control) or an N-WASP specific inhibitor, wiskostatin (2 or 5 μM), at day 7 in culture. At day 12 in culture, neurons were fixed and stained for SV2 (Green) and actin using rhodamine-conjugated phalloidin (Red). Bar = 10 μm. Enlargements of dendrites are shown below the panels. Bar = 2 μm. A dose dependent decrease in the number of SV2 clusters and dendritic spines was observed. Differences between control-2 μM, control-5 μM, and 2-5 μM were statistically significant as determined by Student's *t* test (* and **, $P < 0.0001$). For each condition, at least 40 dendrites from at least 20 neurons were analyzed. Error bars represent SEM from at least three separate experiments.

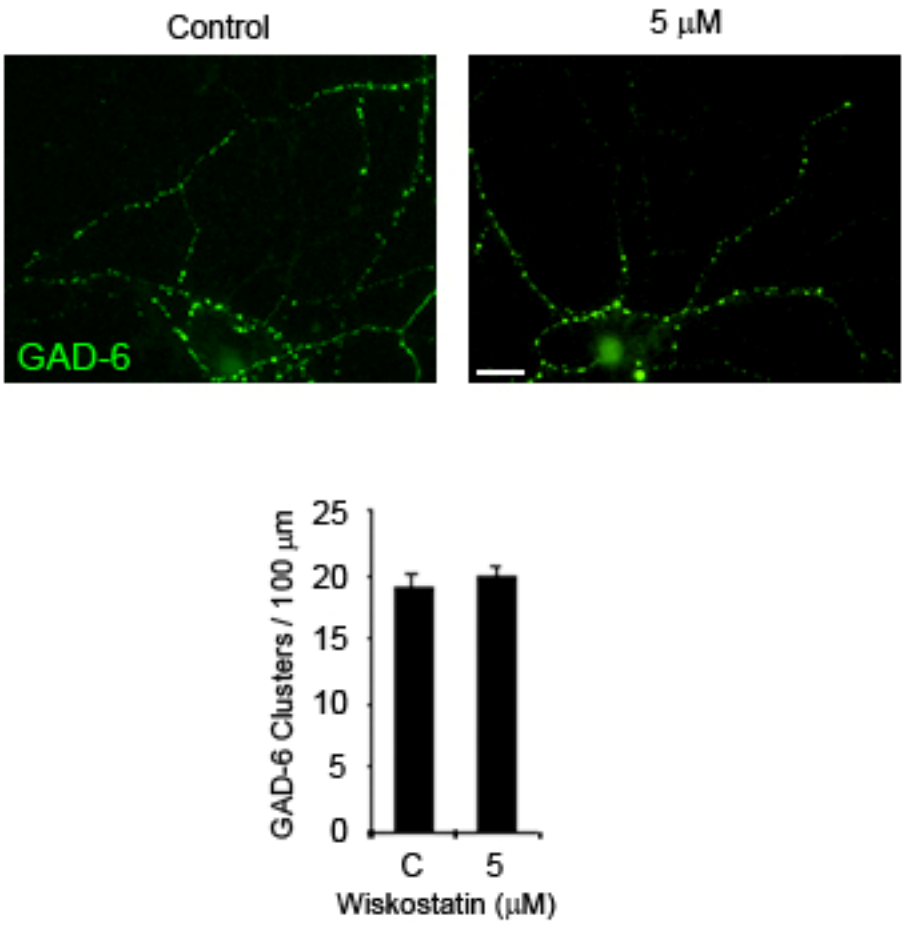

FIGURE 11. Inhibition of N-WASP activity by wiskostatin has no effect on inhibitory synapses.

Hippocampal neurons were treated with either DMSO (Control) or an N-WASP specific inhibitor, wiskostatin (5 μM), at day 7 in culture. At day 12 in culture, neurons were fixed and stained for PSD-95. Bar = 10 μm. Wiskostatin did not significantly affect the number of inhibitory synapses as shown by immunostaining for GAD-6. For each condition, at least 40 dendrites from at least 20 neurons were analyzed. Error bars represent SEM from at least three separate experiments.

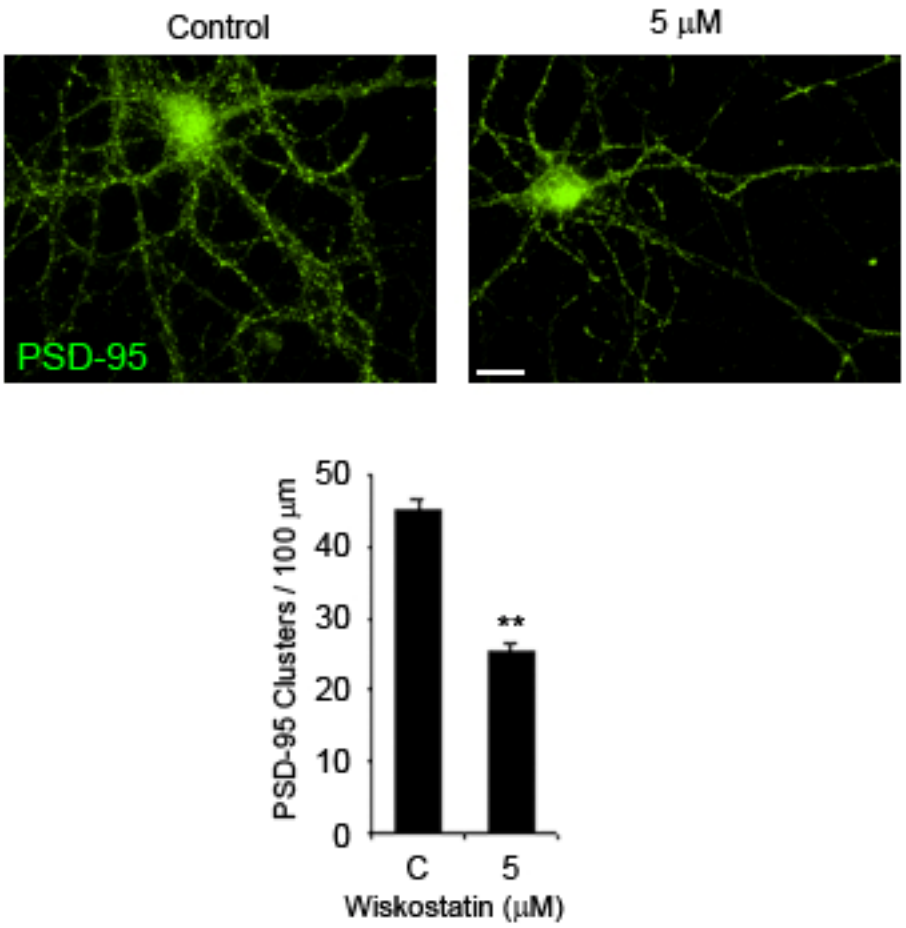

Figure 12. Inhibition of N-WASP activity by wiskostatin decreases excitatory synapses.

Hippocampal neurons were treated with either DMSO (Control) or an N-WASP specific inhibitor, wiskostatin (5 μM), at day 7 in culture. At day 12 in culture, neurons were fixed and stained for PSD-95. Bar = 10 μm. A significant decrease in the number of excitatory synapses (** $P < 0.0001$), as shown by a reduction in the density of PSD-95 clusters, was observed with 5 μM wiskostatin treatment.. For each condition, at least 40 dendrites from at least 20 neurons were analyzed. Error bars represent SEM from at least three separate experiments.

growth of axons or dendrites were seen at any of the wiskostatin concentrations used.

Interestingly, we noticed that at the highest concentration of wiskostatin (5 μM) many of the remaining synapses were concentrated around the neuronal cell bodies. It has previously been reported that inhibitory GABAergic synapses are most dense around the cell body and form directly on the dendrite or cell soma surface without a spine (Craig et al., 1994), which led us to look further at the type of synapses that were regulated by N-WASP activity. To examine the effect of wiskostatin treatment on inhibitory synapses, we used a GAD-6 antibody to assess the density of GABAergic synapses. There was no significant difference in the number of inhibitory synapses with wiskostatin treatment (Figure 11), indicating that N-WASP activation is not necessary for the formation of these synapses. By contrast, wiskostatin treatment had a significant effect on the synaptic density of excitatory glutamatergic synapses as the number of PSD-95 puncta was decreased by more than 50% (Figure 12). Since excitatory synapses can form on dendritic spines or on the dendritic shaft, we assessed the effects of wiskostatin treatment on each of these types of excitatory synapses. Wiskostatin treatment decreased the number of excitatory synapses that formed on spines by almost 90% (20.4 ± 1.7 in controls vs. 2.3 ± 0.6 in wiskostatin treated), but had no significant effect on shaft synapses (20.2 ± 1.7 in controls vs. 19.6 ± 1.6 in wiskostatin treated). In these experiments, neurons were treated for 5 days with wiskostatin to ensure that N-WASP activity was inhibited during a critical time when many spines and synapses form. However, treatment of the neurons for a shorter period of time also resulted in a significant decrease in the number of spines and synapses. We added 5 μm wiskostatin to the neuronal cultures at day 7, washed out the wiskostatin at day 8, and stained for

PSD-95 and phalloidin at day 12. This one day wiskostatin treatment caused a 51% decrease in the number of spines (17.9 ± 1.0 in controls vs. 8.7 ± 0.6 in wiskostatin treated) and a 30% reduction in the number of synapses (37.5 ± 1.8 in controls vs. 26.2 ± 1.7 in wiskostatin treated). Taken together, our results suggest that activation of N-WASP is important for the regulation of spine morphogenesis and the formation of excitatory glutamatergic synapses.

We generated an RNAi construct to knockdown expression of endogenous N-WASP to further explore the role of N-WASP in dendritic spine and synapse formation. The RNAi sequence had been previously shown to be specific for N-WASP and to almost completely knock down expression of the protein (Kawamura et al., 2004; Kempiak et al., 2005; Yamaguchi et al., 2005). However, we confirmed the ability of the RNAi construct to specifically knock down rat N-WASP expression by transiently transfecting it into HEK-293T cells along with GFP-tagged rat N-WASP or WAVE1. As determined by immunoblot analysis, the N-WASP RNAi construct decreased expression of N-WASP by greater than 85% compared to empty pSUPER vector (Figure 13, left panels). In contrast, a scrambled RNAi control had no effect on expression of N-WASP (Figure 13, right panels). The N-WASP RNAi construct did not affect expression of WAVE1, another WASP family member, indicating its specificity for N-WASP (Figure 13, middle panels). The RNAi construct was similarly effective in decreasing expression of N-WASP in the neurons. Transfection of neurons with N-WASP RNAi resulted in an 87.2 ± 4.8% decrease in N-WASP expression compared with control cultures. When neurons were transfected with the N-WASP RNAi construct at day 6 and fixed and stained for SV2 and PSD-95 at day 12, a significant decrease in the number of dendritic spines and

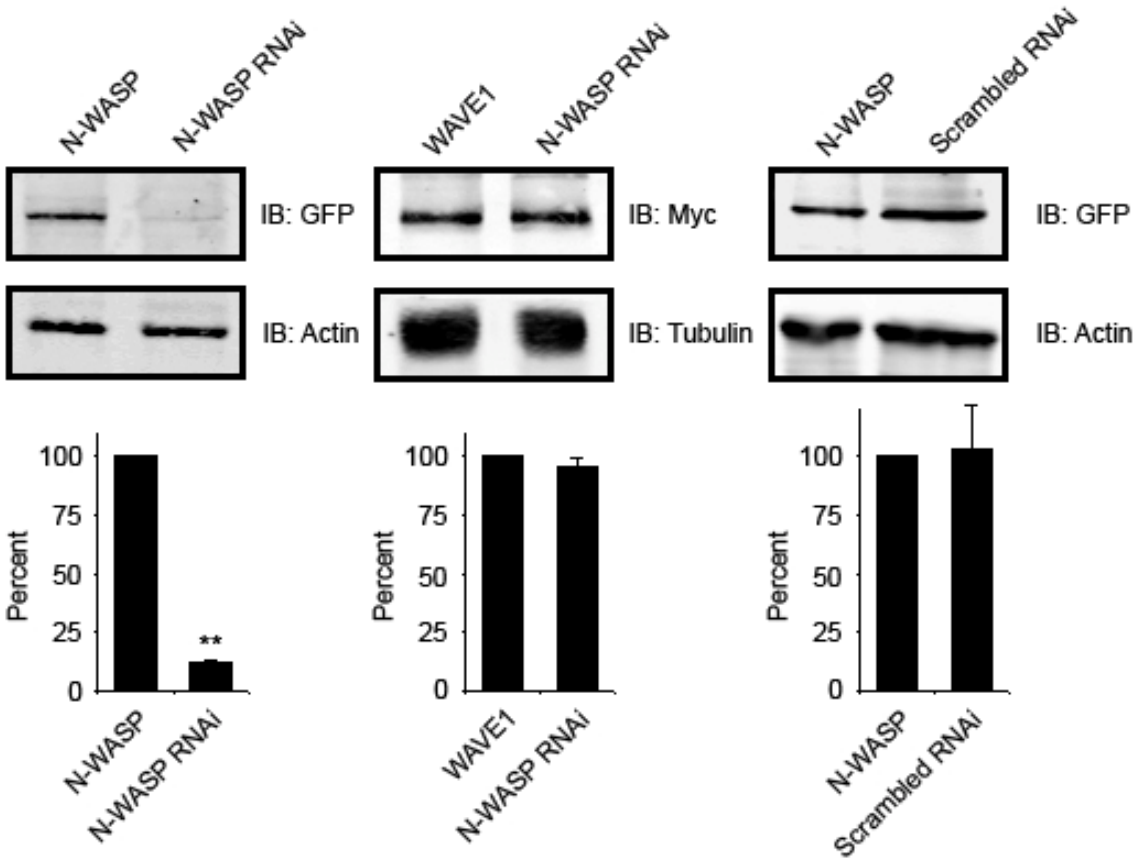

Figure 13. Specific knockdown of N-WASP in HEK-293 cells.

HEK-293T cells were co-transfected with N-WASP RNAi or empty pSUPER vector and either GFP-N-WASP or myc-WAVE1. For a nonsilencing control, a scrambled RNAi construct was prepared and tested by co-transfection with GFP-N-WASP into HEK-293T cells. The lysates were blotted for GFP and β-actin or myc and α-tubulin. The N-WASP RNAi construct specifically decreased N-WASP expression by 85% (left panels), but did not alter expression of WAVE1 (middle panels), another WASP family member. The scrambled RNAi construct did not affect expression of N-WASP (right panels). Quantification of blots from three separate experiments is shown (lower panels).

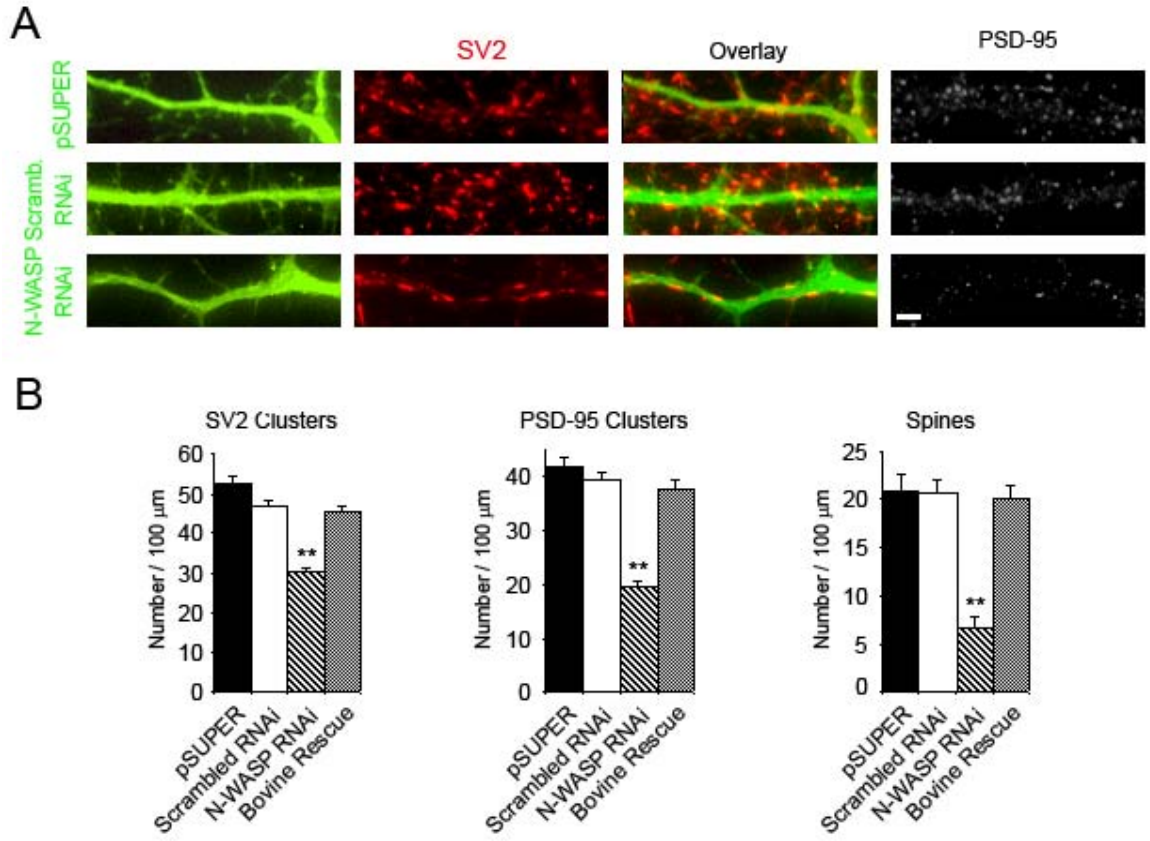

Figure 14. Knockdown of endogenous N-WASP affects spines and synapses in hippocampal neurons.

A, hippocampal neurons were co-transfected with GFP and either empty pSUPER vector, scrambled RNAi, or the N-WASP RNAi construct at day 6 in culture, fixed at day 12 in culture, and stained for the synaptic markers SV2 (middle panels and overlay) and PSD-95 (right panels). A significant decrease in the number of spines and synapses was observed in neurons expressing N-WASP RNAi compared with either scrambled RNAi or pSUPER controls. Bar = 2 μM. B, quantification of the number of spines and synapses (SV2 and PSD-95 clusters) in neurons transfected with empty pSUPER vector, N-WASP RNAi, or scrambled RNAi is shown (** P value < 0.0001). The N-WASP RNAi mediated defects on spines and synapses was rescued by expression of bovine N-WASP (Bovine Rescue). For each condition, at least 40 dendrites from at least 20 neurons from three different cultures were analyzed. Error bars represent SEM from at least three separate experiments.

synapses was observed compared with cells expressing a scrambled RNAi construct or empty pSUPER vector (Figure 14 A and B). To further show that the effects of N-WASP RNAi were specifically attributable to the loss of N-WASP, rescue experiments were performed in which bovine N-WASP was co-expressed with N-WASP RNAi. The rat N-WASP RNAi target sequence does not significantly affect expression of bovine N-WASP due to several nucleotide mismatches (Yamaguchi et al., 2005). Expression of bovine N-WASP almost completely rescued the N-WASP RNAi-mediated defect in spine and synapse formation (Figure. 14B). These results suggest that the defect is due to the loss of endogenous N-WASP and point to an important role for N-WASP in spine and synapse formation.

The Actin and Arp2/3 Binding Domains of N-WASP are Critical for its Function in Regulating Spine and Synapse Formation

We next used several deletion constructs of N-WASP to determine the domains of the protein necessary for spine and synapse formation. For these experiments, the synaptic density was determined by staining for both SV2 and PSD-95, and the number of spines was assessed by GFP fluorescence as well as staining with phalloidin. Phalloidin, which binds F-actin and is commonly used to visualize dendritic spines (Allison et al., 1998; Fischer et al., 1998), was used to assess spine density, since it is possible that the GFP tagged fragments of N-WASP differentially localize to spines. Interestingly, similar results for the spine density were observed with both methods.

The C-terminus of N-WASP is composed of two verprolin homology (V) domains, which bind G-actin, a central (C) domain, and an acidic (A) region that binds the Arp2/3 complex (Figure15) (Machesky et al., 1999; Rohatgi et al., 1999). The VCA region of N-

WASP, which we refer to as “WA”, is sufficient to stimulate the nucleation of new actin filaments by the Arp2/3 complex (Machesky et al., 1999; Rohatgi et al., 1999). Expression of GFP-N-WASP caused a small but significant increase in the density of dendritic spines and synapses compared to GFP alone (Figure 16 A and B). Expression of N-WASP lacking the C-terminal VCA region (ΔWA) significantly decreased the number of spines and synapses compared to control neurons expressing GFP, but protrusions were still observed along the dendrites of N-WASP-ΔWA-expressing neurons (Figure 16A and B). Protrusions were defined as extensions from the dendrites without associated synapses while dendritic spines were in contact with presynaptic terminals. In contrast, expression of N-WASP lacking the N-terminal WH1 region (ΔWH1) did not significantly affect the density of spines or synapses as compared to controls (Figure 16A and B). These results suggest that activation of the Arp2/3 complex by N-WASP promotes spine and synapse formation in the neurons and could be a mechanism by which dendritic spine heads enlarge and subsequently mature.

To further explore the function of the WA region in spine and synapse formation, we transfected neurons with a construct encoding the C-terminal region (WA) of N-WASP. Expression of the WA region resulted in a slight decrease in the density of spines and synapses. In neurons expressing the WA region, a 14% decrease in the number of spines as determined by staining with phalloidin, and a 25% reduction in the synaptic density (PSD-95 clusters) was observed when compared with cells expressing GFP alone (Figure 16A and B). However, significantly more spines and synapses were observed in neurons expressing the WA region than with cells expressing truncated N-WASP that lacked the C-terminal WA region, suggesting that the WA region of N-WASP is critical for its

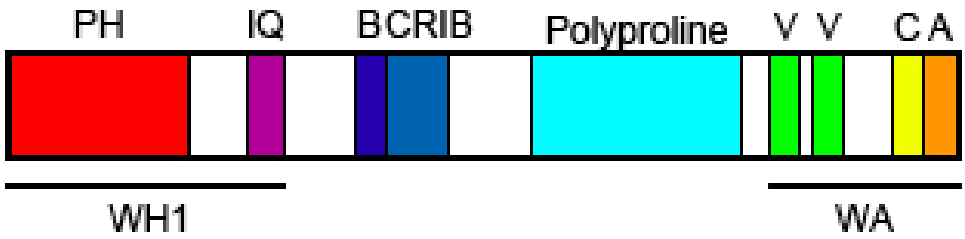

Figure 15. Domain Structure of N-WASP.

Domain structure of N-WASP. Pleckstrin homology (PH), calmodulin binding (IQ), basic (B), Cdc42/Ras interactive binding (CRIB), verprolin homology (V), central (C), and acidic (A) domains are shown.

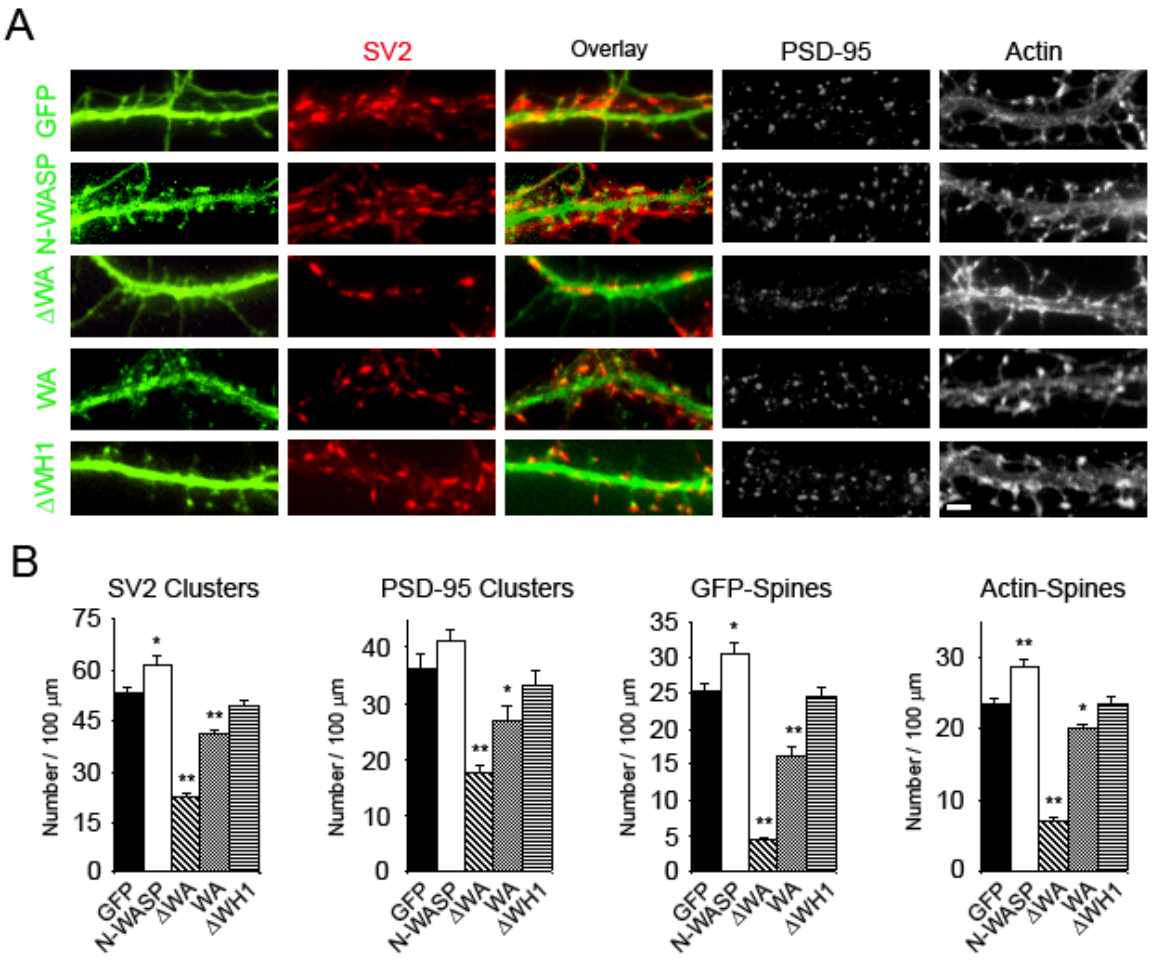

Figure 16. N-WASP binding to actin and the Arp2/3 complex is important for dendritic spine and synapse formation.

A, hippocampal neurons were transfected with GFP, GFP-N-WASP, GFP-N-WASP-ΔWA, GFP-N-WASP-WA, and GFP-N-WASP-ΔWH1 at day 5 in culture, fixed, and immunostained for SV2, PSD-95, and actin (phalloidin) at day 12 in culture. Expression of N-WASP slightly increased the density of spines and synapses, while deletion of the C-terminal WA region from N-WASP significantly decreased the number of spines and synapses. Bar = 2 µm. B, quantification of SV2 and PSD-95 clusters and dendritic spines using GFP fluorescence and by staining for actin (phalloidin) from transfected neurons is shown. Asterisks denote statistically significant differences when compared to control GFP expression neurons (* $P < 0.025$, ** $P < 0.0001$). For each condition, at least 40 dendrites from at least 20 neurons from three different cultures were analyzed. Error bars represent SEM from at least three separate experiments.

function in spine and synapse formation. Taken together, our results strongly suggest that activation of the Arp2/3 complex by N-WASP is critical for the formation of dendritic spines and synapses.

Cdc42 Plays a Role in the Development of Dendritic Spines and Synapses

Since the Rho family GTPase Cdc42 is a known activator of N-WASP (Symons et al., 1996), we explored its function in regulating spine and synapse formation by preparing an RNAi construct to knock down expression of Cdc42 in neurons. We tested the ability of the Cdc42 RNAi construct to knock down expression of the endogenous protein by transfecting it into Rat2 fibroblasts. Immunoblot analysis showed that the RNAi construct decreased expression of Cdc42 by greater than 75% compared to control pSUPER vector (Figure 17, left panels). By contrast, a scrambled RNAi construct did not significantly affect expression of Cdc42 (Figure 17, right panels). When neurons were transfected with the Cdc42 RNAi construct, a significant decrease in the number of spines and synapses was observed compared to cells transfected with a scrambled RNAi construct or empty pSUPER vector (Figure 18A and B). A similar decrease in the density of spines and synapses was seen in neurons expressing dominant negative Cdc42 (DN-Cdc42) (Figure 18A and B). The Cdc42 RNAi-mediated defect in spine and synapse formation could be rescued, at least partially, by expression of the WA region of N-WASP, linking Cdc42 to N-WASP activation in the development of spines and synapses (Figure 18A and B).

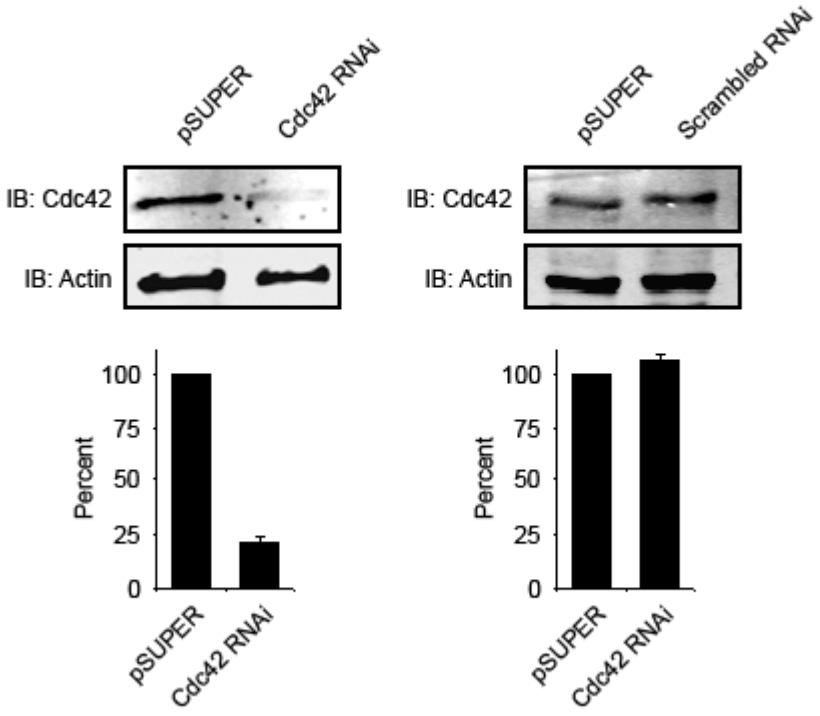

Figure 17. Knockdown of endogenous Cdc42 in Rat2 Fibroblasts.

A, Rat2 fibroblasts were co-transfected with GFP and either Cdc42 RNAi, scrambled RNAi, or empty pSUPER vector. The lysates were blotted for Cdc42 and actin as a loading control. Expression of the Cdc42 RNAi construct decreased endogenous levels of Cdc42 by greater than 75% (left panels) while the scrambled RNAi construct did not affect Cdc42 expression (right panels). Quantification of blots from three separate experiments is shown (lower panels).

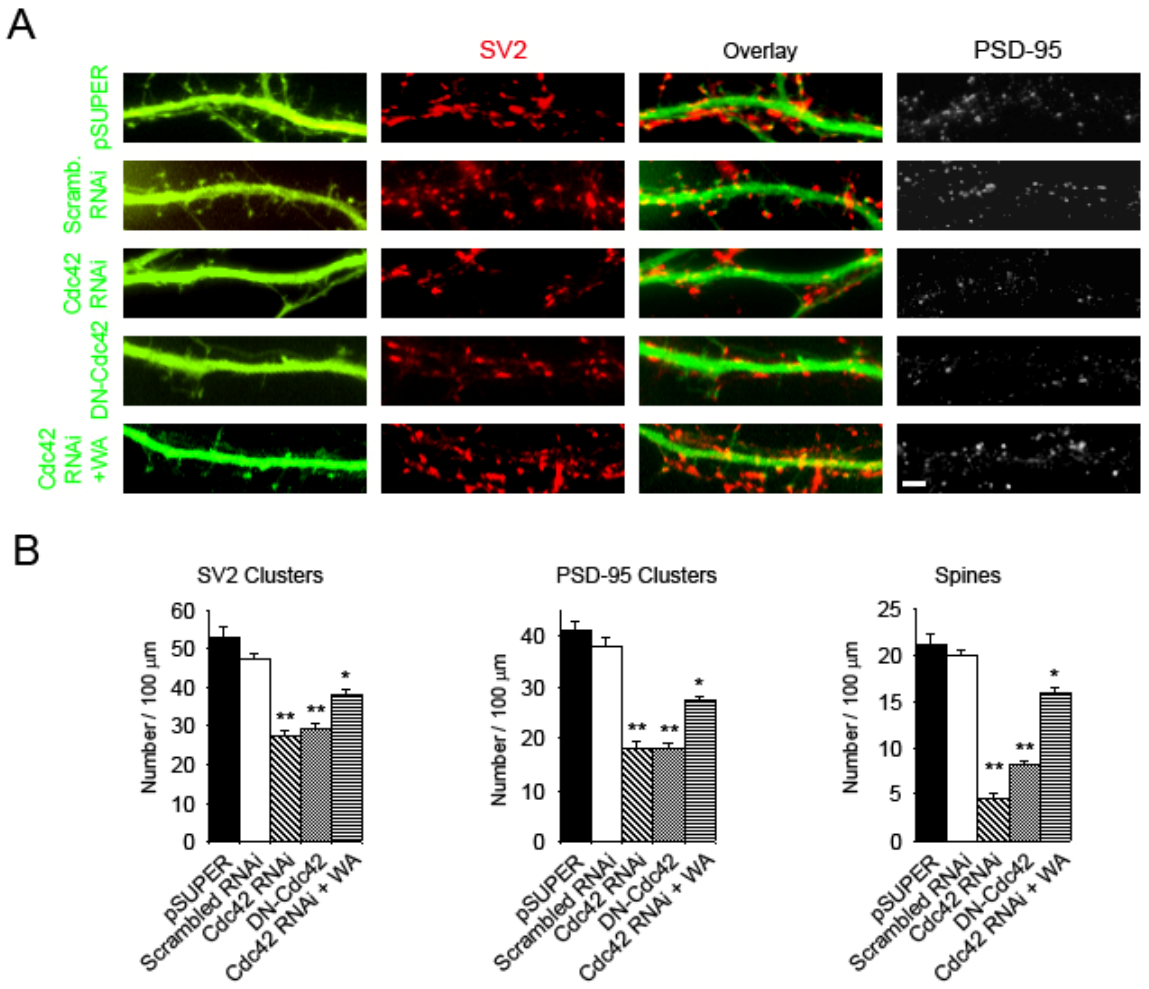

Figure 18. Cdc42 plays a role in the development of dendritic spines and synapses.

A, hippocampal neurons were co-transfected with GFP and either empty pSUPER vector, scrambled RNAi, Cdc42 RNAi, or dominant negative Cdc42 (DN-Cdc42) and stained for the synaptic markers SV2 (middle panels) and PSD-95 (right panels). A significant decrease in the density of spines and synapses was observed in neurons expressing Cdc42 RNAi compared with either scrambled RNAi or pSUPER controls. A similar defect in the formation of spines and synapses was seen in neurons expressing dominant negative Cdc42. When neurons were co-transfected with Cdc42 RNAi and a GFP tagged WA construct, the defects on spines and synapses associated with knockdown of Cdc42 were partially reversed by expression of the WA region of N-WASP. Bar = 2 µM. B, quantification of the number of spines and synapses (SV2 and PSD-95 clusters) in neurons transfected with empty pSUPER vector, scrambled RNAi, Cdc42 RNAi, DN-Cdc42, or Cdc42 RNAi + GFP-WA is shown. Differences between control-Cdc42 RNAi, control-DN-Cdc42 (** P value < 0.0001) and Cdc42 RNAi-Cdc42RNAi + GFP-WA (* P value < 0.0001) were statistically significant. For each condition, at least 40 dendrites from at least 15 neurons from three different cultures were analyzed. Error bars represent SEM from at least three separate experiments.

Arp3 Regulates the Formation of Spines and Synapses in Hippocampal Neurons

Since our results strongly implicated the Arp2/3 complex as a downstream effector of N-WASP in spine and synapse formation, we examined its subcellular localization in hippocampal neurons. GFP- tagged Arp3, one of the seven proteins found in the Arp2/3 complex, localized in puncta along neuronal processes with the synaptic markers SV2 and PSD-95, suggesting that it was synaptic (Figure 19, arrows). A similar localization was observed by immunostaining for endogenous Arp3 and SV2 (Figure 19). Higher magnification images showed that Arp3 puncta were in close apposition to SV2 clusters and completely merged with PSD-95 puncta, indicating that Arp3, like N-WASP, is enriched on the postsynaptic side of excitatory synapses (Figure 19).

Since Arp3 localized to spines and excitatory synapses, we generated an RNAi construct to examine its function in regulating the formation of these structures. Although the RNAi sequence had been previously shown to effectively knock down expression of Arp3 (Steffen et al., 2006), we tested its ability to knock down rat Arp3 by transfecting it into HEK-293T cells with GFP-tagged Arp3. The Arp3 RNAi construct decreased expression of Arp3 by almost 80% while a scrambled RNAi control did not affect Arp3 expression (Figure 20). When neurons were transfected with the Arp3 RNAi construct, a significant decrease in the number of spines and synapses was observed compared with control cultures expressing scrambled RNAi or empty pSUPER vector (Figure. 21). The decrease in the density of spines and synapses in neurons expressing the Arp3 RNAi construct was similar to that observed when N-WASP expression was knocked down in these cells. Thus, our results suggest that N-WASP and the Arp2/3 complex are important regulators in the formation of dendritic spines and synapses.

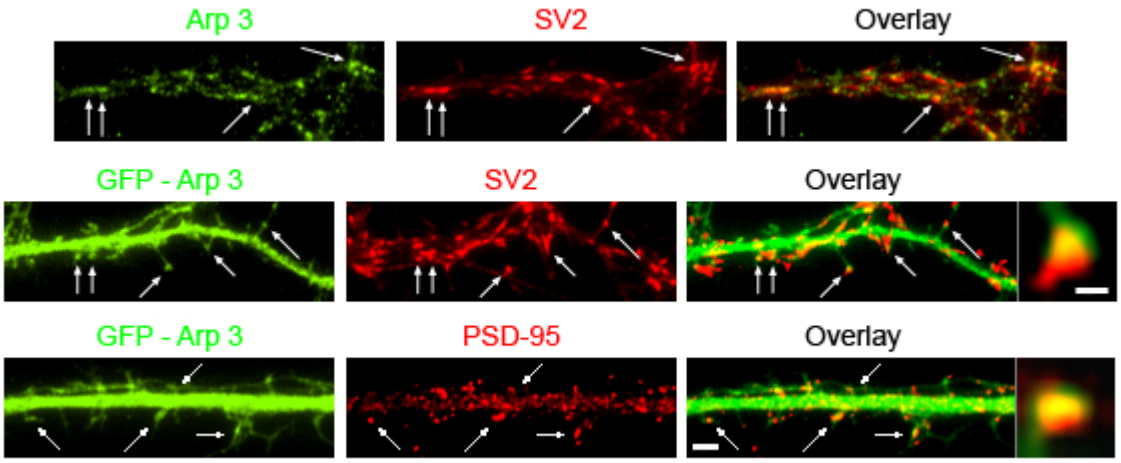

Figure 19. Endogenous and GFP-Arp3 localizes to spines and synapses in hippocampal neurons .

Hippocampal neurons at day 14 in culture were co-immunostained for endogenous Arp3 (upper panels) and the synaptic marker SV2. Endogenous Arp3 accumulated in puncta with SV2 (overlay, arrows). Hippocampal neurons were transfected with GFP-Arp3 at day 5 in culture, fixed, and immunostained for SV2 (middle panels) and PSD-95 (lower panels) at day 12 in culture. GFP-Arp3 localized in puncta along neuronal processes with SV2 and PSD-95 (overlays, arrows). Bar = 2 μm. High magnification images showed Arp3 puncta were in close apposition to SV2 and completely merged with PSD-95, indicating that Arp3 is enriched in the postsynaptic side of excitatory synapses. Bar = 0.4 μm.

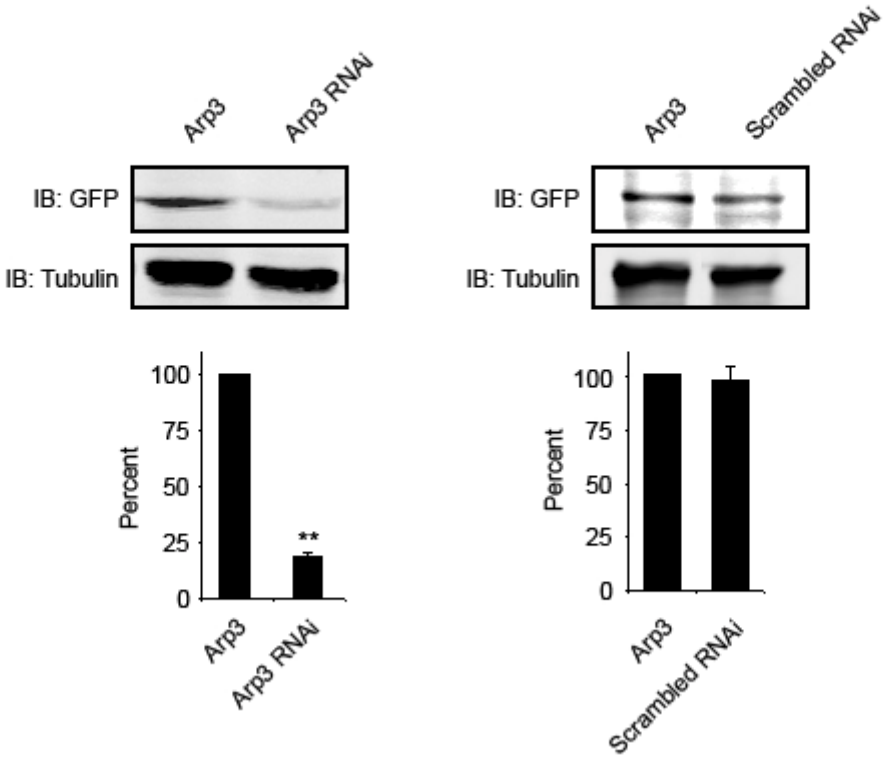

Figure 20. Knockdown of Arp3 in HEK-293 cells .

HEK-293T cells were co-transfected with Arp3 RNAi, scrambled RNAi, or empty pSUPER vector and GFP-Arp3. The lysates were blotted for GFP and α-tubulin. The Arp3 RNAi construct decreased expression of Arp3 by almost 80% (left panels) while the scrambled RNAi did not alter Arp3 expression (right panels). Quantification of blots from three separate experiments is shown (lower panels).

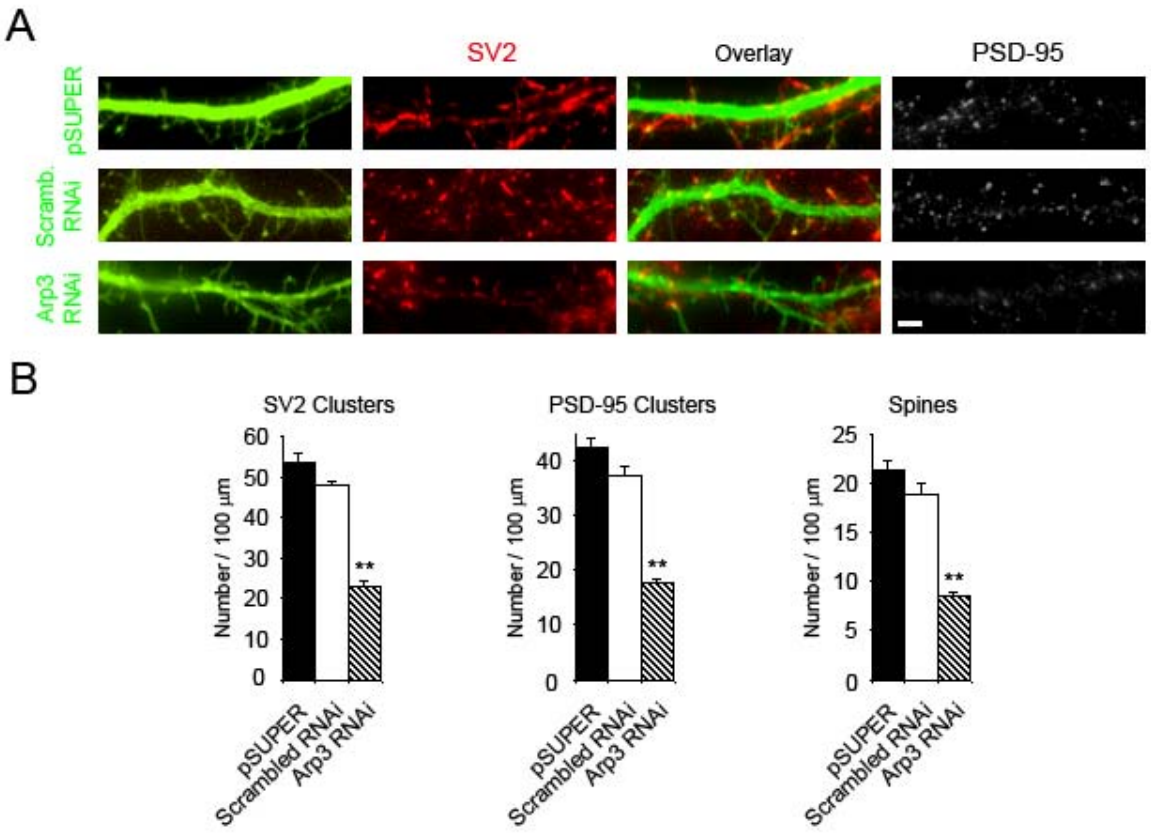

Figure 21. The Arp2/3 complex regulates the formation of dendritic spines and synapses in hippocampal neurons.

A, hippocampal neurons were co-transfected with GFP and either empty pSUPER vector, scrambled RNAi, or the Arp3 RNAi construct at day 6 in culture, fixed at day 12, and stained for the synaptic markers SV2 (middle panels) and PSD-95 (right panels). A significant decrease in the density of spines and synapses was observed in neurons expressing Arp3 RNAi compared with either scrambled RNAi or pSUPER controls. Bar = 2 µM. B, quantification of the number of spines and synapses (SV2 and PSD-95 clusters) in neurons transfected with empty pSUPER vector, scrambled RNAi, or Arp3 RNAi is shown (** P value < 0.0001). For each condition, at least 40 dendrites from at least 15 neurons from three different cultures were analyzed. Error bars represent SEM from at least three separate experiments.

Discussion

Our results reveal a novel mechanism by which N-WASP activation of the Arp2/3 complex regulates the formation of dendritic spines and synapses in hippocampal neurons. N-WASP is enriched in spines and excitatory synapses that are active and functional as determined by loading with FM4-64 dye. Knockdown of endogenous N-WASP resulted in a significant decrease in the density of spines and synapses. The C-terminal region of the protein, which binds and activates the Arp2/3 complex, is critical for this function of N-WASP. Knockdown of Arp3, an important protein in the Arp2/3 complex, caused a similar defect in the formation of spines and synapses, pointing to the significance of activation of the Arp2/3 complex in this process. An activator of N-WASP, Cdc42, is also involved in regulating spine and synapse formation. Knockdown of Cdc42 expression resulted in a significant decrease in the number of spines and synapses and expression of the WA region of N-WASP rescued the Cdc42-mediated defect in spine and synapse formation, suggesting that activation of N-WASP by Cdc42 is important in this process. Thus, our study provides a molecular mechanism by which N-WASP and an activator and effector regulate the development of dendritic spines and synapses.

The function of Cdc42 in regulating the development of spines and synapses is presently unclear. Recent studies have indicated a role for Cdc42 in dendritic morphogenesis in *Drosophila* and learning-related synaptic growth in *Aplysia* sensory neurons (Scott et al., 2003; Udo et al., 2005). In addition, activation of Cdc42 is proposed to be an important event in converting nonfunctional contacts into functional synapses (Shen et al., 2006). However, others have suggested that Cdc42 does not have a

significant effect on the maintenance of dendritic spine morphology in hippocampal neurons (Govek et al., 2004; Tashiro et al., 2000). Our results are consistent with Cdc42 regulating the formation of dendritic spines and synapses. The previous studies in hippocampal neurons relied on expression of constitutively active and dominant negative Cdc42 mutants after many spines and synapses had formed (day 10-12 in culture) while our study used RNAi to specifically knock down Cdc42 expression during a time when many spines and synapses are actively forming (day 5-6 in culture). It may be difficult to see a dramatic effect of Cdc42 on spines and synapses after a significant number of the spines and synapses have already formed.

Our results show that the spine and synaptic density in the WA-expressing neurons was slightly decreased compared with neurons expressing full-length N-WASP. It was previously reported that the WA region alone is much more potent in stimulating actin polymerization by the Arp2/3 complex than full length N-WASP (Rohatgi et al., 1999). Delocalized reorganization of actin may limit the amount of G-actin and Arp2/3 complex available for actin assembly at synaptic sites, which could diminish the ability of spines to stabilize and mature. Consistent with this, aberrant actin reorganization has been reported to result in a decrease in the density of spines and synapses in neurons (Zhang et al., 2003; Zhang et al., 2005).

Aside from regulating actin polymerization for the control of cell morphology, N-WASP has also been linked to several steps in vesicular trafficking including clathrin-mediated endocytosis, golgi trafficking, and synaptic vesicle endocytosis in neurons (Matas et al., 2004; Merrifield et al., 2004; Shin et al., 2007). The actin polymerization mediated by N-WASP and the Arp2/3 complex is thought to drive movement of vesicles.

It is possible that N-WASP plays a dual role in regulating spine and synapse formation through both the underlying actin cytoskeleton as well as through neuronal vesicle trafficking. Further studies will be required to determine the role of N-WASP mediated trafficking in the formation and morphology changes of dendritic spines.

The process of spine formation has received a great deal of interest because of the importance of these structures in cognitive function, but the molecular mechanisms that regulate spine formation still remain poorly understood. Our results suggest that activation of the Arp2/3 complex by N-WASP is critical for the formation of dendritic spines and synapses. This raises the question of how the Arp2/3 complex functions in spine and synapse formation. While the exact steps in spinogenesis are not clear, it appears that spines can either form from dendritic protrusions or extend directly from the dendritic shaft (Dailey and Smith, 1996; Ethell and Pasquale, 2005; Fiala et al., 1998; Marrs et al., 2001; Ziv and Smith, 1996). In both cases, the spine head enlarges or expands as the spine matures and the Arp2/3 complex mediated branching of actin may play an important role in this process. When activation of the Arp2/3 complex by N-WASP is inhibited, the formation of dendritic spines is impaired. Activation of the Arp2/3 complex may form a branched actin network that promotes and supports the enlargement and maturation of the spine head. This branched actin network may also be important for the morphological changes in spines associated with synaptic plasticity. Future studies are needed to better understand the complex regulation of actin and its contribution to the formation and plasticity of spines and synapses.

In summary, we show that activation of N-WASP regulates the formation of dendritic spines and synapses through the Arp2/3 complex. The activation of the Arp2/3

complex could stimulate spine development by forming a branched actin network that promotes the enlargement of spine heads, which subsequently lead to their maturation.

CHAPTER IV

WAVE1 IN SPINE AND SYNAPSE FORMATION

Introduction

WAVE1, 2, and 3 have all been implicated in the development of overall neuronal morphology as well as the formation of spines and synapses. Expression of WAVE1 and 3 is restricted to the brain, while WAVE2 is expressed ubiquitously (Nagase et al., 1996; Suetsugu et al., 1999). Initial studies carried out in the neuroblastoma NG108 cell line showed differential distribution of the three WAVEs in the neuronal growth cone, suggesting that they may all potentially play a role in neurite outgrowth. WAVE1 localized to the leading edge but not filopodia, while WAVE2 & 3 continuously localized to the tips of filopodia and the initiation sites of microspikes (Nozumi et al., 2003). The WHD/SHD domains were required for their localization.

Although WAVE1 is primarily expressed in the brain (Nagase et al., 1996), its function in the nervous system is not completely understood. In this study, we show that WAVE1 is essential for the formation of dendritic spines and synapses in hippocampal neurons. This activity of WAVE1 is dependent on its C-terminal binding and activation of the Arp2/3 complex. Inhibition of Arp2/3 binding to WAVE1 resulted in a significant reduction in the density of spines and synapses, pointing to a critical role for WAVE1 acting through the Arp2/3 complex in the development of dendritic spines and synapses in the CNS.

Experimental Procedures

Reagents

SV2 (1:250) monoclonal antibody was from the Developmental Studies Hybridoma Bank (The University of Iowa, Iowa City, IA). Alexa Fluor® 555 anti-mouse for immunohistochemistry was from Molecular Probes (Eugene, OR).

Plasmids

The small interfering RNA (RNAi) construct was prepared by ligating annealed sense and antisense 64mer-oligonucleotides into pSUPER vector as previously described (Zhang and Macara, 2008). The WAVE1 RNAi oligo contained the following 19 nucleotide target sequence: 5'-AGAAGAACTGTCCTTACAA-3'. GFP-WAVE1-ΔWA, -ΔA, and -WA were generous gifts from Timothy Vartanian (Beth Israel Deaconess Medical Center, Boston, MA).

Results

Since our results with the N-WASP deletion mutants suggested that the Arp2/3 complex plays an important role in spine and synapse formation, we examined another WASP family member, WAVE1, which signals through the Arp2/3 complex. We expressed C-terminal deletion mutants of WAVE1, as well as the full length protein, to further examine the function of Arp2/3 complex in spine and synapse formation in the neurons. Expression of full length WAVE1 resulted in a slight increase in the number of spines and synapses (Figure 22). In contrast, WAVE1-ΔWA, similar to N-WASP-ΔWA (Figure 16), caused a significant decrease in the density of spines and synapses compared

with full length WAVE1 (Figure 22). Interestingly, a mutant only lacking the acidic (A) region at the extreme C-terminal end of WAVE1, which binds Arp2/3 complex, caused a similar decrease. Expression of the WA region of WAVE1 alone caused a slight but significant decrease in spines and synapses, again similar to what was seen with neurons expressing the WA region of N-WASP (Figure 16). Thus, our results strongly suggest that activation of the Arp2/3 complex by the WASP family is critical for the formation of dendritic spines and synapses.

To further test the hypothesis that WAVE1 is involved in spine and synapse formation, we generated an RNAi construct to knockdown expression of endogenous WAVE1. We confirmed the ability of the RNAi construct to knock down rat WAVE1 expression by transiently transfecting it into HEK-293T cells along with GFP-tagged rat WAVE1. As determined by immunoblot analysis, the WAVE1 RNAi construct decreased expression of WAVE1 by greater than 80% compared to empty pSUPER vector (Figure 23). When neurons were transfected with the WAVE1 RNAi construct at day 6 and fixed and stained for SV2 at day 12, a significant decrease in the number of dendritic spines (21.36 ± 1.14 to 4.98 ± 0.53) and synapses (53.63 ± 2.29 to 32.94 ± 2.01) was observed compared with cells expressing empty pSUPER vector (Figure 24) ($p < 0.0001$).

Discussion

This data provides further evidence for WASP family activation of the Arp2/3 complex in the formation of dendritic spines. Using the WAVE1-ΔA construct, we were able to more specifically target the WAVE1 interaction with the Arp2/3 complex without

disrupting the V domain, which is responsible for G-actin binding. Elimination of Arp2/3 binding, while leaving the V domain intact, has a significant impact on the number of dendritic spines in hippocampal neurons, indicating that binding of WAVE1 to monomeric actin alone is not sufficient for the formation of dendritic spines. It is not surprising that there is no difference in the number of spines and synapses between neurons expressing the ΔA and ΔWA mutants, because both completely disrupt WAVE1 activation of Arp2/3 complex.

This data raises several questions about the roles of WAVE1 and N-WASP signaling through Arp2/3 in the development of spines and synapses. The RNAi mediated knockdown of either protein individually, as well as the elimination of binding to Arp2/3 by either proteins, results in a similar phenotype, indicating that both are necessary for the formation of dendritic spines and synapses. This suggests two possibilities. Either they are both members of a linear pathway that results in spine formation, or both proteins are involved in non-redundant parallel pathways that are activated either by the same signal or independent signals and converge on Arp2/3. Further study is necessary to determine which possibility is the case.

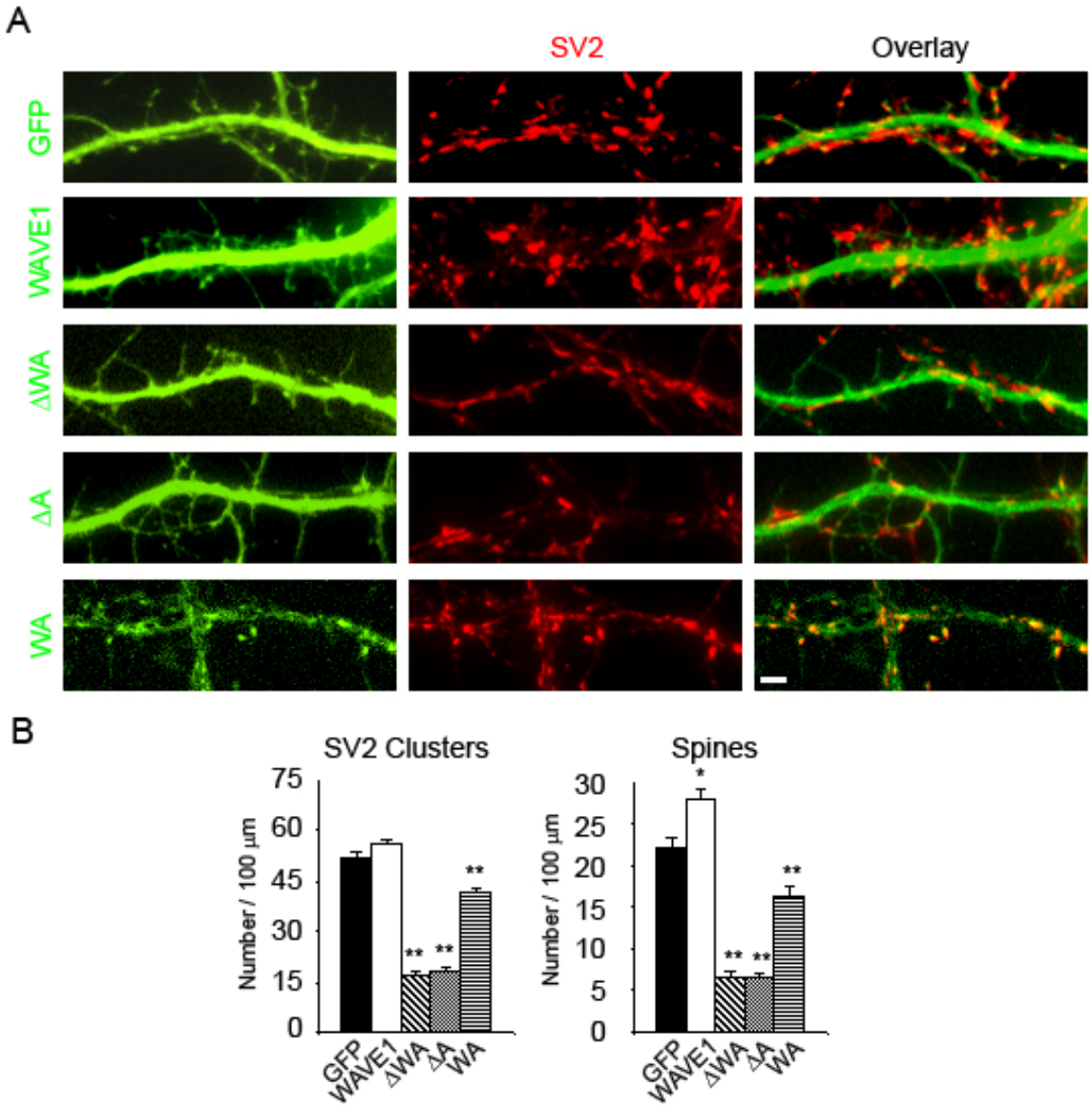

Figure 22. WAVE1 binding to actin and the Arp2/3 complex is important for dendritic spine and synapse formation.

A, hippocampal neurons were transfected with GFP, GFP-WAVE1, GFP-WAVE1-ΔWA, GFP-WAVE1-ΔA, and GFP-WAVE1-WA at day 5 in culture, fixed, and immunostained for SV2 at day 12 in culture. Expression of WAVE1 slightly increased the density of spines and synapses, while deletion of the C-terminal WA or A region from WAVE1 significantly decreased the number of spines and synapses. Bar = 2 µm. B, quantification of SV2 and PSD-95 clusters and dendritic spines using GFP fluorescence from transfected neurons is shown. Asterisks denote statistically significant differences when compared to control GFP expression neurons (* P <0.025, ** P < 0.0001). For each condition, at least 40 dendrites from at least 20 neurons from three different cultures were analyzed. Error bars represent SEM from at least three separate experiments.

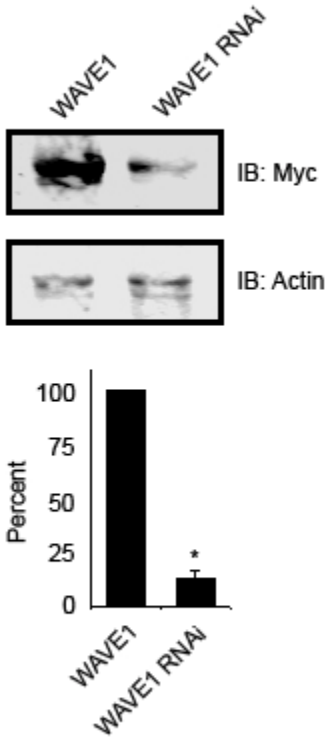

Figure 23. Knockdown of WAVE1 in HEK-293 cells .

HEK-293T cells were co-transfected with WAVE1 RNAi or empty pSUPER vector and myc-WAVE1. The lysates were blotted for myc and actin. The WAVE1 RNAi construct decreased expression by more than 80%. Quantification of blots from three separate experiments is shown (lower panels).

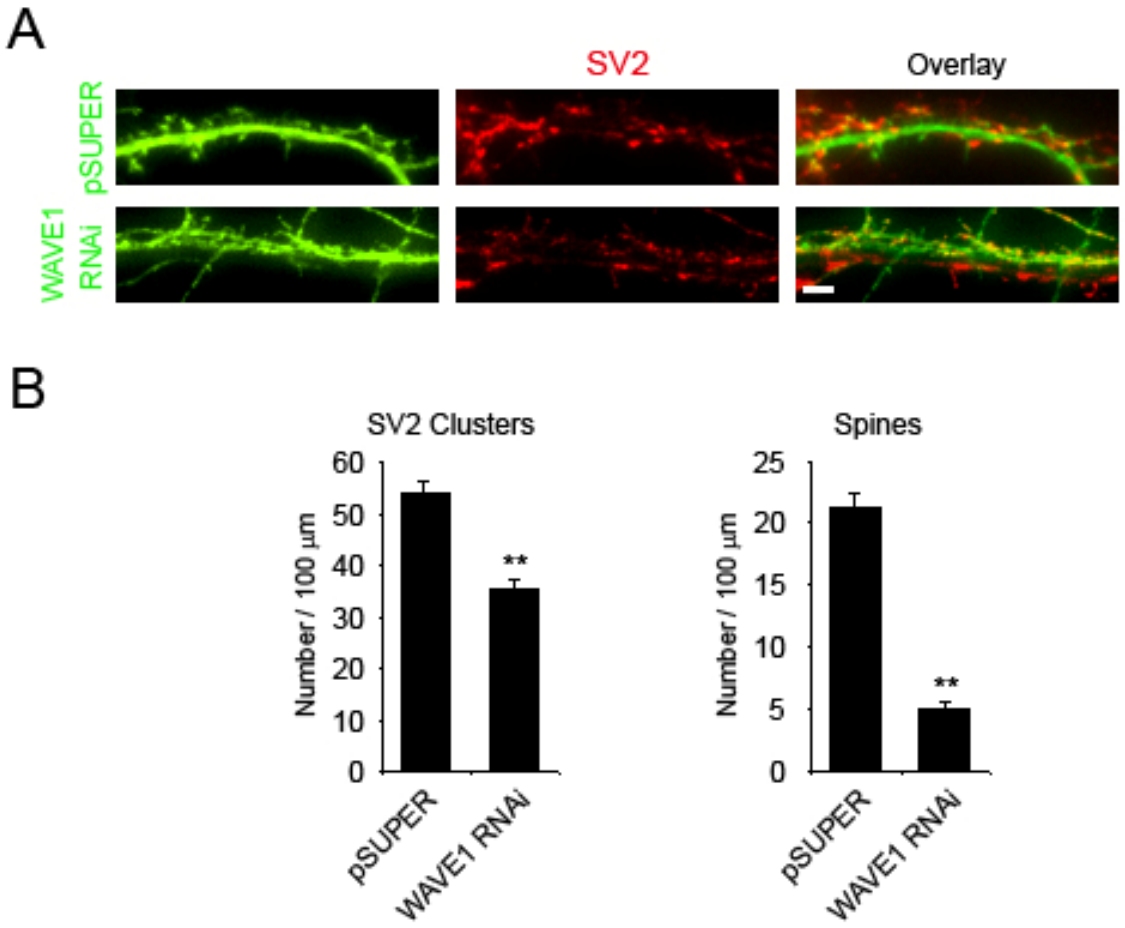

Figure 24. Knockdown of endogenous WAVE1 affects spines and synapses in hippocampal neurons.

A, hippocampal neurons were co-transfected with GFP and either empty pSUPER vector or the WAVE1 RNAi construct at day 6 in culture, fixed at day 12 in culture, and stained for the synaptic markers SV2 (middle panels and overlay). A significant decrease in the number of spines and synapses was observed in neurons expressing WAVE1 RNAi compared with pSUPER controls. Bar = 2 µM. B, quantification of the number of spines and synapses (SV2 clusters) in neurons transfected with empty pSUPER vector or N-WASP RNAi is shown (** P value < 0.0001) For each condition, at least 20 dendrites from at least 10 neurons from three different cultures were analyzed. Error bars represent SEM from at least three separate experiments.

CHAPTER V

CONCLUSIONS AND FUTURE DIRECTIONS

We have shown that activation of the Arp2/3 complex by the WASP family member N-WASP is necessary for the formation of dendritic spines and synapses in cultured rat hippocampal neurons. N-WASP localized to the postsynaptic side of active synapses as shown by multiple synaptic markers. In this location, it is in position to initiate polymerization of new actin filaments through Arp2/3 complex activation that could provide the driving force to shape the head of a maturing dendritic spine. Inhibition of N-WASP activity, either through pharmacological inhibition by wiskostatin or RNAi mediated knockdown, resulted in a significant decrease in the number of both spines and synapses, indicating that N-WASP activity is necessary for the generation of dendritic spines and, as a result, the synapses associated with those spines. Expression of N-WASP deletion constructs showed the importance of N-WASP binding to the Arp2/3 complex, as deletion of the WA region of N-WASP, implicated in the activation of the Arp2/3 complex, significantly decreased the number of spines and synapses. Activation of N-WASP by Cdc42 is also an important step in the formation of dendritic spines and synapses, as RNAi mediated knockdown of Cdc42 mimics the phenotype of N-WASP knockdown, and this defect in the number of spines can be partially rescued by expression of the constitutively active WA region of N-WASP. The Arp2/3 complex localizes to spines and synapses, as shown by Arp2/3 localization with several synaptic markers, where it is in position to be activated by N-WASP in the maturation of dendritic

spines. RNAi mediated knockdown of Arp2/3 showed a similar decrease in the number of spines and synapses as seen with Cdc42 and N-WASP knockdown. However, many more filopodial like dendritic spine precursors were seen in these experiments, indicating that N-WASP may act through another downstream effector aside from Arp2/3 to induce the initial protrusion of spine precursors.

Future Directions

Although we have presented evidence suggesting that Cdc42 acts upstream of N-WASP in a pathway that regulates spine formation, future studies will be needed to determine the factors which initiate this signaling cascade. Transmembrane receptors that are activated when the dendritic spine comes into contact with its presynaptic partner provide one possibility. Two receptors involved in cell-cell adhesions, which have previously been shown to be involved in dendritic spine formation, are α5 integrin and the EphB receptor (Irie and Yamaguchi, 2004; Webb et al., 2007). Both have been linked to activation of Rho family GTPases and remodeling of the actin cytoskeleton in neurons (Huber et al., 2003), and could potentially lead to activation of N-WASP in the formation of dendritic spines.

A majority of the experiments performed here involved manipulations beginning at day 6 in culture and continuing until the neurons were fixed at day 12 in culture. Wiskostatin was applied and constructs were transfected at this time in order to allow for adequate neurite outgrowth before affecting actin polymerization, and to insure they were present at the critical time when spines and synapses were beginning to form. This leaves

the question of exactly what time during the development of a neuron as well as what stage of dendritic spine development N-WASP activity is required. Other proteins have been shown to have differential temporal requirements in the development in spines and synapse. Rac activity was required throughout the life of the spine, while the adaptor protein GIT1 was only required during the early stages of spine development (Zhang et al., 2003). We saw an affect on the number of synapses when wiskostatin was applied for one day at day 8 in culture, but these experiments could be expanded to other time periods and different points during neuronal development. Neurons could also be left in culture for longer than 12 days to assess the affect of manipulations on synapses formed later in the development of a neuron and maintenance of previously formed spines. Application of wiskostatin at later time points could also indicate whether N-WASP is involved in maintenance of the structure of already developed spines.

Stimulation of neurons is known to cause formation of new spines and remodeling of already existing spines, and both processes require reorganization of the actin cytoskeleton (Matus, 2000). Protocols utilizing glutamate stimulation or depolarization by high levels of K+ could be used to study requirements of N-WASP for formation and remodeling of spines (Pilpel and Segal, 2005; Sung et al., 2008). We would expect to see N-WASP localize to new dendritic spines as well an increase in N-WASP in spines undergoing depolarization or stimulation mediated morphological changes. If N-WASP is involved in rapid reorganization of the cytoskeleton during depolarization mediated plasticity, N-WASP could be linked to synaptic plasticity, the process thought to underlie learning and memory formation (Engert and Bonhoeffer, 1999).

All of the data to this point which implicates N-WASP in dendritic spine formation has been from dissociated cultured hippocampal neurons. These experiments should be repeated under conditions more similar to an *in vivo* environment. Hippocampal slices provide a model system that is more like the *in vivo* environment, but are still accessible for imaging and electrophysiological experiments and are transfectable. Transfection of the N-WASP RNAi construct, as well as the corresponding deletion mutants eliminating Arp2/3 binding, could be transfected into slices, and the experiments looking at dendritic spine and synapse formation in the cultured neurons could be recapitulated in the slice. The electrophysiological properties of the slices could also be studied to determine if N-WASP plays a role in neural connectivity and induction of LTP and LTD.

APPENDIX A

DETAILED SYNAPSE COUNTING PROTOCOL

1. Open desired image in MetaMorph.
2. Perform “Count Nuclei” calibration as outlined in Appendix B.
    a. The preliminary setting shown below in the “Count Nuclei” box in step 8 may also be used and adjusted as needed (see note after step 11).
3. Click “Measure,” then “Region Measurements.” The “Region Measurements” window will appear.

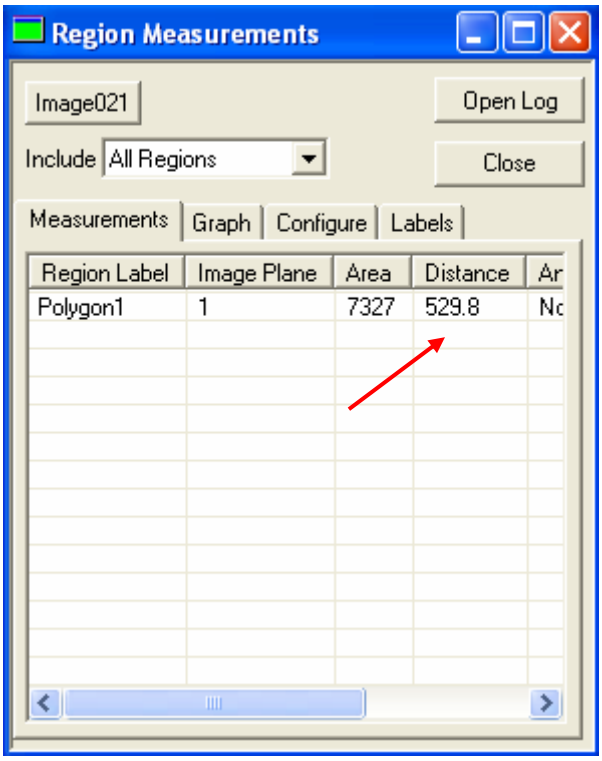

4. Click the polygonal outlining button on the drawing toolbar and trace the desired region on the image.

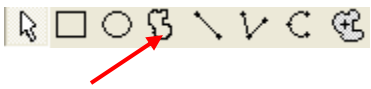

5. The distance of the line will be visible in the "Region Measurements" window, and will be used later to calculate the number of synapses per 100 microns.
    a. Click the "Configure" tab to choose which values are shown (area, distances, etc).
6. With the desired region highlighted (selected with a dancing line), choose "Edit," then "Duplicate," then "Image." A new window will appear with only the selected region. This window will be named "Copy of XXX."
    a. It is important to note that while overlay images may be copied in this fashion, regions from overlay images *cannot* be used with the "Count Nuclei" Application.
7. Choose "Apps," then "Count Nuclei." The Count Nuclei window will appear.

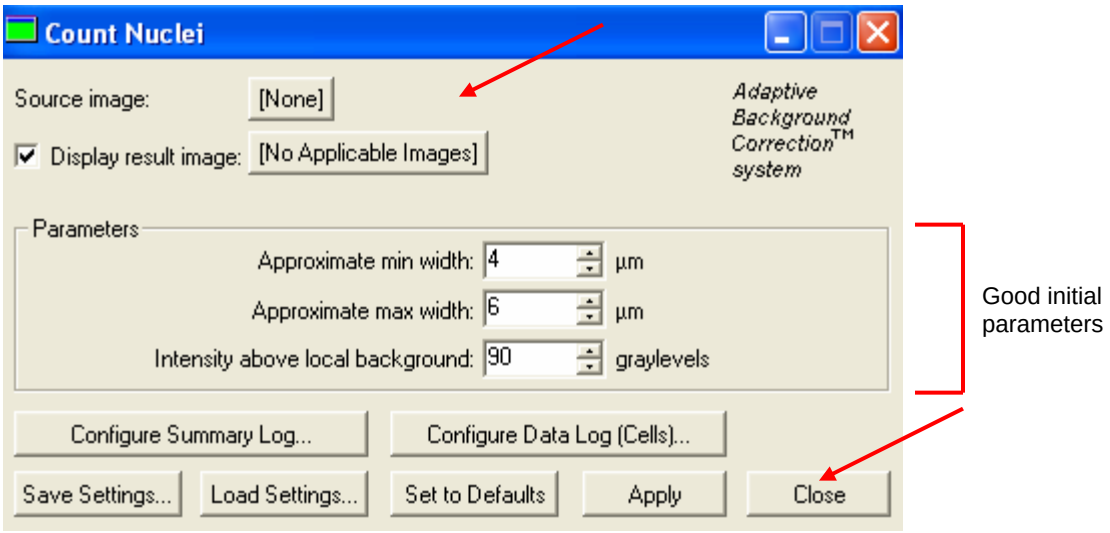

8. Click the "Source Image" button, then select "Copy of XXX" from the dropdown list. The most recently made copy will appear at the top of the list.
    a. To count the spots on an entire image (not just a specific region), skip steps 3-7 and choose the desired image from the "Source Image" dropdown tab.
9. Click "Apply."

10. Two new windows will appear, a “Cellular Results for Count Nuclei” and a “Segmentation” window.
    a. The “Cellular Results for Count Nuclei” (scrolling down, if necessary) will indicate the number of synapses. Each spot recognized is given its own number, so the largest number assigned is equal to the total number of spots.
    b. The “Segmentation” window shows the spots recognized by the program, which also appear on the original “Copy of XXX” image window as an overlay.

Note: *The max and min width values need to be increased or decreased in the “Parameters” section of the “Count Nuclei” box often. Generally, while the intensity value set during initial calibration will hold for an entire set of pictures, the max/min values will not. Always manually check the overlay to see if the program is counting spots that should or should not be counted.*

Data Analysis in Excel

1. The sample Excel spreadsheet below show how to determine the number of spots per 100µm. Data gathered from MetaMorph will be put into the first two columns. The final three columns will be calculated by Excel.

A	B	C	D	E
Number of spots *(from step 9a)*	Total Length of Line Drawn *(from step 3)*	= B/2 (*Length of dendrite)*	=C * 0.2159 *(pixels to µm conversion)*	= A/D * 100 *(synapses/100 µm)*

    a. 0.2159 is the conversion constant for the 60X objective from pixels to µm.

b. The value in column C is the length of the dendrite counted. While this is not exactly the perimeter of the dendrite (column B) divided by 2, a considerable amount of time is saved with this method, and does not significantly affect the data. The actual length may be determined using the line tool, but this adds an extra step.

APPENDIX B

"COUNT NUCLEI" MODULE INSTRUCTIONS

Molecular Devices

Using the Count Nuclei application module in MetaMorph version 6.3 and higher

ABSTRACT

This document describes how to use the Count Nuclei Assay using the Count Nuclei application module from the Apps menu in MetaMorph version 6.3 or higher.

This document describes the following procedures:

- Configuring the assay and saving settings
- Running the module and logging measurement data

ARTICLE #
T20042

PRODUCTS
MetaMorph® 6.3 and higher

CREATED
28-Jul-2005

LAST UPDATED
23-Sep-2005

NOTES

- For more information about the procedures and dialog boxes described in this document, refer to the MetaMorph Help by pressing the [F1] key within the software to view the help information about the active dialog box. You can also click the *See Also* button from within the Help window for additional information such as dialog box settings.
- This document assumes that the Count Nuclei drop-in has been loaded using the Meta Imaging Series Administrator.

GETTING STARTED

1. Start MetaMorph.
2. Open a nuclei image of interest.

FIGURE 1
NUCLEI IMAGE

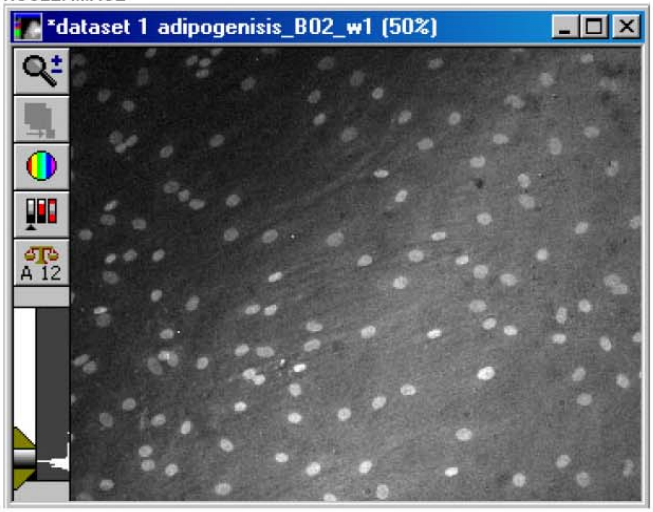

CONFIGURING THE COUNT NUCLEI ASSAY

1. From the Apps Menu, select Count Nuclei. The Count Nuclei dialog box opens, as shown in Figure 2:

FIGURE 2
COUNT NUCLEI DIALOG BOX

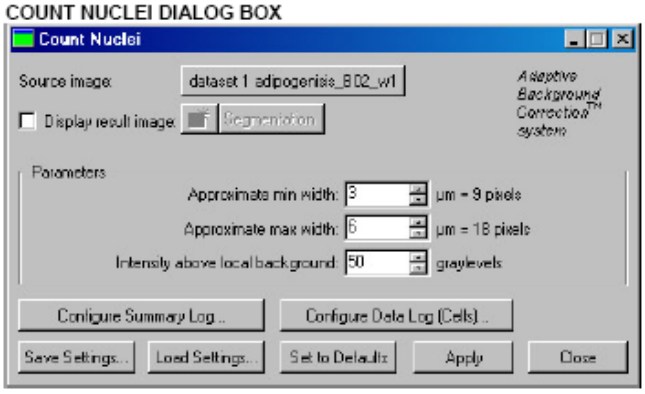

2. Click *Source Image:* and select the image of interest. Valid source images are 16-bit images.
3. Optionally, check the box next to *Display result image*. This option will create a new result image called *Segmentation* after the analysis is run. You can change the result image name by clicking the *Segmentation* image selector and clicking *Specified*. The result image shows segmentation of the nuclei drawn as different indexed colors according to nucleus size on a black background.
4. From the Region Menu, select Region Tools. The Region toolbar should appear if it is not already present.
5. Select the Single Line tool, as shown in Figure 3:

FIGURE 3
REGION TOOLS DIALOG BOX – SELECTING THE SINGLE LINE TOOL

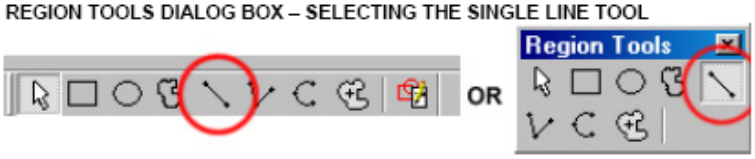

6. On the image, locate one of the narrowest nuclei.
7. Zoom in, move the mouse pointer to one edge of the cell and left-click to start the line.
8. Move the mouse pointer to the other edge and read the value shown right after *Length*. In Figure 4, the value is 9 pixels or 2.89 microns (this sample image is calibrated). Left-click again to set the line:

FIGURE 4
MEASURING THE NUCLEI

9. In the Count Nuclei dialog box, in the *Approximate Min Width* field, type the nucleus width in microns. The value for the number of pixels is displayed outside the box to the right.
10. Repeat steps 7-9 for one of the widest nuclei. Enter this measurement in the *Count Nuclei* dialog box, in the *Approximate Max Width* box. You can remove the regions of interest in the image by selecting Clear Regions from the Region Menu.

    NOTE: Another way to measure the width of an object is with calipers. For more information on calipers, see the *Additional Information* section at the end of this document.

11. Click the Arrow tool on the Region toolbar.
12. Find one of the dimmest nuclei.
13. Move the mouse pointer over the nucleus and read the gray value displayed at the bottom of the screen. The gray value in Figure 5 is 330:

FIGURE 5
GRAY VALUE DISPLAYED AT THE BOTTOM OF THE SCREEN

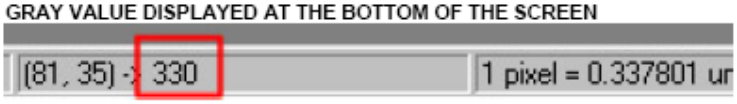

14. Move the mouse pointer just outside the nucleus to measure the background.
15. Calculate the difference between the nucleus signal and the background. In this example the background was approximately 290. The difference between the gray value of the nucleus and the gray value of the background is 330 - 290 = **40**.
16. Select a slightly lower value than 40 and type it in the *Intensity above local background* field of the Count Nuclei dialog box. In this example, a value of 35 was used.
17. Click *Apply* to evaluate your settings. The Cellular Results table opens, as well as a segmentation image window (if the option *Display result image* is checked). The gray value of the nuclei on the segmentation image refers to the cell's assigned label number as it appears in the Cellular Results table. The assigned label is based on cell area and numbered according to increasing cell area measurements. The original image also will have an overlay that can be toggled on and off using the *Show/Hide Overlay* button on the image window, as shown in Figure 6:

FIGURE 6
THE SHOW/HIDE OVERLAY BUTTON ON THE IMAGE WINDOW

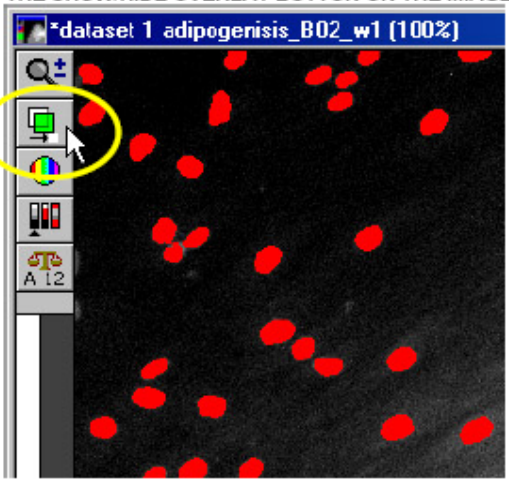

18. Click the *Show/Hide Overlay* button to see if all the nuclei are detected or if too much background was detected. Possible problems:
    a. Not all nuclei were found: try lowering the *Intensity above local background* or if only large nuclei were found, try decreasing the *Approximate min width*.

b. Too much background was included with your nuclei: try raising the Intensity *above local background* or try decreasing the *Approximate max width*.
c. If nuclei are split into pieces: try increasing the *Approximate min width*.

19. Repeat steps 12-18 until the appropriate results are obtained.
20. To log the summary data, select the *Log* menu, select *Open Summary Log*, check the box next to *Dynamic Data Exchange (DDE)* if using Microsoft® Excel®, and click *OK*. The Export Log Data dialog box opens. Click *OK* to open Excel.
21. In the Count Nuclei dialog box, click *Configure Summary Log*. The Configure Log dialog box opens. Check and/or uncheck individual measurement parameters and logging options. Refer to the description of these settings under *Dialog Box Options: Configure Summary Log* in the Help file, accessible by pressing the [**F1**] key. Click *OK* to close the Configure Log dialog box.
22. To log individual cell data, select the *Log* menu, *Open Data Log*, check the box next to *Dynamic Data Exchange (DDE)* if using Microsoft® Excel®, and click *OK*. The Export Log Data dialog box will open. Click *OK* to open Excel.
23. In the Count Nuclei dialog box, click *Configure Data Log (Cells)* The Configure Log dialog box opens. Check and/or uncheck individual measurement parameters and logging options. Refer to the description of these settings under *Dialog Box Options: Configure Data Log (Cells)* in the Help file, accessible by pressing the [**F1**] key. Click *OK* to close the Configure Log dialog box.
24. In the Count Nuclei dialog box, click *Save Settings* to name and save your settings for future use.
25. In the Count Nuclei dialog box, click *Apply* to evaluate the measurements and export the data to Excel.
26. Change settings if needed and resave the settings.
27. You can now run the settings on other images by clicking *Load Settings* in the Count Nuclei dialog box.

ADDITIONAL INFORMATION

You can also use the Caliper tool to measure the width of an object. The caliper function is a drop-in that must be loaded into the software. If the command is not present in the *Measure* menu, please see your System Administrator to load it. Complete the following procedure to use the *Calipers* tool:

1. From the Measure menu, select Calipers. The Calipers dialog box opens.
2. Select the image to measure in the *Image* selector. The caliper appears on the selected image, as shown in Figure 7:

FIGURE 7
CALIPERS DIALOG BOX

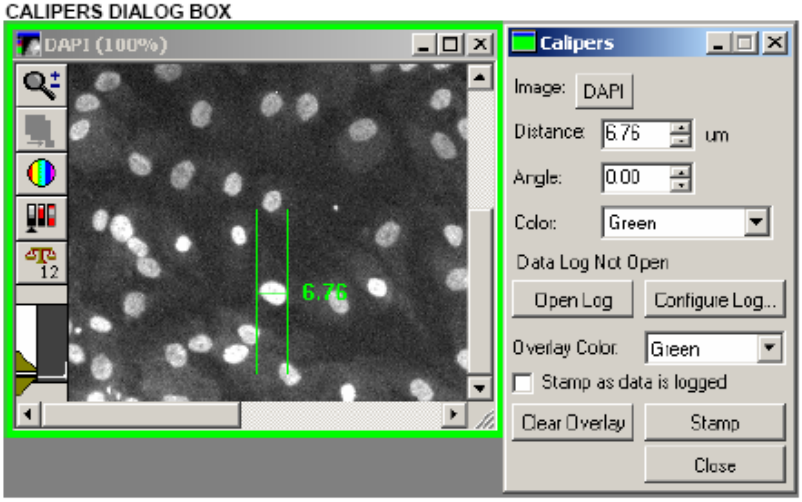

3. The calipers can be moved by single-clicking the cross-bar so that it is displayed as a blinking line, indicating that it is active, and then dragging (or rotating) the cross-bar to the desired location with your pointer.
4. Enter the value in the *Approximate max width* field of the application module dialog box.

REFERENCES

Abe, T., M. Kato, H. Miki, T. Takenawa, and T. Endo. 2003. Small GTPase Tc10 and its homologue RhoT induce N-WASP-mediated long process formation and neurite outgrowth. *J Cell Sci*. 116:155-68.

Allison, D.W., V.I. Gelfand, I. Spector, and A.M. Craig. 1998. Role of actin in anchoring postsynaptic receptors in cultured hippocampal neurons: differential attachment of NMDA versus AMPA receptors. *J. Neurosci.* 18:2423-36.

Amann, K.J., and T.D. Pollard. 2001. Direct real-time observation of actin filament branching mediated by Arp2/3 complex using total internal reflection fluorescence microscopy. *Proc Natl Acad Sci U S A*. 98:15009-13.

Anton, I.M., and G.E. Jones. 2006. WIP: a multifunctional protein involved in actin cytoskeleton regulation. *Eur J Cell Biol*. 85:295-304.

Aronheim, A., Y.C. Broder, A. Cohen, A. Fritsch, B. Belisle, and A. Abo. 1998. Chp, a homologue of the GTPase Cdc42Hs, activates the JNK pathway and is implicated in reorganizing the actin cytoskeleton. *Curr Biol*. 8:1125-8.

Aspenstrom, P. 2002. The WASP-binding protein WIRE has a role in the regulation of the actin filament system downstream of the platelet-derived growth factor receptor. *Exp Cell Res*. 279:21-33.

Aspenstrom, P., U. Lindberg, and A. Hall. 1996. Two GTPases, Cdc42 and Rac, bind directly to a protein implicated in the immunodeficiency disorder Wiskott-Aldrich syndrome. *Curr Biol*. 6:70-5.

Bacon, C., V. Lakics, L. Machesky, and M. Rumsby. 2007. N-WASP regulates extension of filopodia and processes by oligodendrocyte progenitors, oligodendrocytes, and Schwann cells-implications for axon ensheathment at myelination. *Glia*. 55:844-58.

Bailly, M., F. Macaluso, M. Cammer, A. Chan, J.E. Segall, and J.S. Condeelis. 1999. Relationship between Arp2/3 complex and the barbed ends of actin filaments at the leading edge of carcinoma cells after epidermal growth factor stimulation. *J. Cell Biol.* 145:331-45.

Banzai, Y., H. Miki, H. Yamaguchi, and T. Takenawa. 2000. Essential role of neural Wiskott-Aldrich syndrome protein in neurite extension in PC12 cells and rat hippocampal primary culture cells. *J Biol Chem*. 275:11987-92.

Betz, W.J., and G.S. Bewick. 1992. Optical analysis of synaptic vesicle recycling at the frog neuromuscular junction. *Science*. 255:200-3.

Betz, W.J., F. Mao, and G.S. Bewick. 1992. Activity-dependent fluorescent staining and destaining of living vertebrate motor nerve terminals. *J. Neurosci.* 12:363-75.

Betz, W.J., F. Mao, and C.B. Smith. 1996. Imaging exocytosis and endocytosis. *Curr. Opin. Neurobiol.* 6:365-71.

Blanchoin, L., K.J. Amann, H.N. Higgs, J.B. Marchand, D.A. Kaiser, and T.D. Pollard. 2000. Direct observation of dendritic actin filament networks nucleated by Arp2/3 complex and WASP/Scar proteins. *Nature*. 404:1007-11.

Bourguignon, L.Y., K. Peyrollier, E. Gilad, and A. Brightman. 2007. Hyaluronan-CD44 interaction with neural Wiskott-Aldrich syndrome protein (N-WASP) promotes actin polymerization and ErbB2 activation leading to beta-catenin nuclear translocation, transcriptional up-regulation, and cell migration in ovarian tumor cells. *J Biol Chem*. 282:1265-80.

Bryan, B., V. Kumar, L.J. Stafford, Y. Cai, G. Wu, and M. Liu. 2004. GEFT, a Rho family guanine nucleotide exchange factor, regulates neurite outgrowth and dendritic spine formation. *J Biol Chem*. 279:45824-32.

Calabrese, B., M.S. Wilson, and S. Halpain. 2006. Development and regulation of dendritic spine synapses. *Physiology (Bethesda)*. 21:38-47.

Carlier, M.F., P. Nioche, I. Broutin-L'Hermite, R. Boujemaa, C. Le Clainche, C. Egile, C. Garbay, A. Ducruix, P. Sansonetti, and D. Pantaloni. 2000. GRB2 links signaling to actin assembly by enhancing interaction of neural Wiskott-Aldrich syndrome protein (N-WASp) with actin-related protein (ARP2/3) complex. *J Biol Chem*. 275:21946-52.

Chereau, D., F. Kerff, P. Graceffa, Z. Grabarek, K. Langsetmo, and R. Dominguez. 2005. Actin-bound structures of Wiskott-Aldrich syndrome protein (WASP)-homology domain 2 and the implications for filament assembly. *Proc Natl Acad Sci U S A*. 102:16644-9.

Choi, J., J. Ko, B. Racz, A. Burette, J.R. Lee, S. Kim, M. Na, H.W. Lee, K. Kim, R.J. Weinberg, and E. Kim. 2005. Regulation of dendritic spine morphogenesis by insulin receptor substrate 53, a downstream effector of Rac1 and Cdc42 small GTPases. *J Neurosci*. 25:869-79.

Cochilla, A.J., J.K. Angleson, and W.J. Betz. 1999. Monitoring secretory membrane with FM1-43 fluorescence. *Annu. Rev. Neurosci.* 22:1-10.

Craig, A.M., C.D. Blackstone, R.L. Huganir, and G. Banker. 1994. Selective clustering of glutamate and gamma-aminobutyric acid receptors opposite terminals releasing the corresponding neurotransmitters. *Proc. Natl. Acad. Sci. U S A*. 91:12373-7.

Dahl, J.P., J. Wang-Dunlop, C. Gonzales, M.E. Goad, R.J. Mark, and S.P. Kwak. 2003. Characterization of the WAVE1 knock-out mouse: implications for CNS development. *J Neurosci*. 23:3343-52.

Dailey, M.E., and S.J. Smith. 1996. The dynamics of dendritic structure in developing hippocampal slices. *J. Neurosci.* 16:2983-94.

Derry, J.M., H.D. Ochs, and U. Francke. 1994. Isolation of a novel gene mutated in Wiskott-Aldrich syndrome. *Cell*. 79:following 922.

Dunaevsky, A., A. Tashiro, A. Majewska, C. Mason, and R. Yuste. 1999. Developmental regulation of spine motility in the mammalian central nervous system. *Proc. Natl. Acad. Sci. U S A*. 96:13438-43.

Eden, S., R. Rohatgi, A.V. Podtelejnikov, M. Mann, and M.W. Kirschner. 2002. Mechanism of regulation of WAVE1-induced actin nucleation by Rac1 and Nck. *Nature*. 418:790-3.

Engert, F., and T. Bonhoeffer. 1999. Dendritic spine changes associated with hippocampal long-term synaptic plasticity. *Nature*. 399:66-70.

Ethell, I.M., and E.B. Pasquale. 2005. Molecular mechanisms of dendritic spine development and remodeling. *Prog. Neurobiol.* 75:161-205.

Fiala, J.C., M. Feinberg, V. Popov, and K.M. Harris. 1998. Synaptogenesis via dendritic filopodia in developing hippocampal area CA1. *J. Neurosci.* 18:8900-11.

Fiala, J.C., J. Spacek, and K.M. Harris. 2002. Dendritic spine pathology: cause or consequence of neurological disorders? *Brain Res. Brain Res. Rev.* 39:29-54.

Fischer, M., S. Kaech, D. Knutti, and A. Matus. 1998. Rapid actin-based plasticity in dendritic spines. *Neuron*. 20:847-54.

Frischknecht, F., V. Moreau, S. Rottger, S. Gonfloni, I. Reckmann, G. Superti-Furga, and M. Way. 1999. Actin-based motility of vaccinia virus mimics receptor tyrosine kinase signalling. *Nature*. 401:926-9.

Fukuoka, M., H. Miki, and T. Takenawa. 1997. Identification of N-WASP homologs in human and rat brain. *Gene*. 196:43-8.

Goldberg, D.J., M.S. Foley, D. Tang, and P.W. Grabham. 2000. Recruitment of the Arp2/3 complex and mena for the stimulation of actin polymerization in growth cones by nerve growth factor. *J Neurosci Res*. 60:458-67.

Goley, E.D., S.E. Rodenbusch, A.C. Martin, and M.D. Welch. 2004. Critical conformational changes in the Arp2/3 complex are induced by nucleotide and nucleation promoting factor. *Mol Cell*. 16:269-79.

Goley, E.D., and M.D. Welch. 2006. The ARP2/3 complex: an actin nucleator comes of age. *Nat Rev Mol Cell Biol*. 7:713-26.

Goslin, K., H. Asmussen, and G. Banker. 1998. Rat hippocampal neurons in low-density culture. MIT Press, Cambridge, MA. pp339-370 pp.

Govek, E.E., S.E. Newey, C.J. Akerman, J.R. Cross, L. Van der Veken, and L. Van Aelst. 2004. The X-linked mental retardation protein oligophrenin-1 is required for dendritic spine morphogenesis. *Nat. Neurosci.* 7:364-72.

Govek, E.E., S.E. Newey, and L. Van Aelst. 2005. The role of the Rho GTPases in neuronal development. *Genes Dev*. 19:1-49.

Govind, S., R. Kozma, C. Monfries, L. Lim, and S. Ahmed. 2001. Cdc42Hs facilitates cytoskeletal reorganization and neurite outgrowth by localizing the 58-kD insulin receptor substrate to filamentous actin. *J Cell Biol*. 152:579-94.

Harris, K.M. 1999. Structure, development, and plasticity of dendritic spines. *Curr. Opin. Neurobiol.* 9:343-8.

Higgs, H.N., and T.D. Pollard. 2000. Activation by Cdc42 and PIP(2) of Wiskott-Aldrich syndrome protein (WASp) stimulates actin nucleation by Arp2/3 complex. *J Cell Biol*. 150:1311-20.

Ho, H.Y., R. Rohatgi, A.M. Lebensohn, M. Le, J. Li, S.P. Gygi, and M.W. Kirschner. 2004. Toca-1 mediates Cdc42-dependent actin nucleation by activating the N-WASP-WIP complex. *Cell*. 118:203-16.

Ho, H.Y., R. Rohatgi, L. Ma, and M.W. Kirschner. 2001. CR16 forms a complex with N-WASP in brain and is a novel member of a conserved proline-rich actin-binding protein family. *Proc Natl Acad Sci U S A*. 98:11306-11.

Huber, A.B., A.L. Kolodkin, D.D. Ginty, and J.F. Cloutier. 2003. Signaling at the growth cone: ligand-receptor complexes and the control of axon growth and guidance. *Annu Rev Neurosci*. 26:509-63.

Hufner, K., H.N. Higgs, T.D. Pollard, C. Jacobi, M. Aepfelbacher, and S. Linder. 2001. The verprolin-like central (vc) region of Wiskott-Aldrich syndrome protein induces Arp2/3 complex-dependent actin nucleation. *J Biol Chem*. 276:35761-7.

Innocenti, M., A. Zucconi, A. Disanza, E. Frittoli, L.B. Areces, A. Steffen, T.E. Stradal, P.P. Di Fiore, M.F. Carlier, and G. Scita. 2004. Abi1 is essential for the formation and activation of a WAVE2 signalling complex. *Nat Cell Biol*. 6:319-27.

Irie, F., and Y. Yamaguchi. 2002. EphB receptors regulate dendritic spine development via intersectin, Cdc42 and N-WASP. *Nat Neurosci*. 5:1117-8.

Irie, F., and Y. Yamaguchi. 2004. EPHB receptor signaling in dendritic spine development. *Front Biosci*. 9:1365-73.

Itoh, T., K.S. Erdmann, A. Roux, B. Habermann, H. Werner, and P. De Camilli. 2005. Dynamin and the actin cytoskeleton cooperatively regulate plasma membrane invagination by BAR and F-BAR proteins. *Dev Cell*. 9:791-804.

Kakimoto, T., H. Katoh, and M. Negishi. 2004. Identification of splicing variants of Rapostlin, a novel RND2 effector that interacts with neural Wiskott-Aldrich syndrome protein and induces neurite branching. *J Biol Chem*. 279:14104-10.

Kakimoto, T., H. Katoh, and M. Negishi. 2006. Regulation of neuronal morphology by Toca-1, an F-BAR/EFC protein that induces plasma membrane invagination. *J Biol Chem*. 281:29042-53.

Kato, M., H. Miki, S. Kurita, T. Endo, H. Nakagawa, S. Miyamoto, and T. Takenawa. 2002. WICH, a novel verprolin homology domain-containing protein that functions cooperatively with N-WASP in actin-microspike formation. *Biochem Biophys Res Commun*. 291:41-7.

Kawamura, K., K. Takano, S. Suetsugu, S. Kurisu, D. Yamazaki, H. Miki, T. Takenawa, and T. Endo. 2004. N-WASP and WAVE2 acting downstream of phosphatidylinositol 3-kinase are required for myogenic cell migration induced by hepatocyte growth factor. *J. Biol. Chem.* 279:54862-71.

Kawano, Y., T. Yoshimura, D. Tsuboi, S. Kawabata, T. Kaneko-Kawano, H. Shirataki, T. Takenawa, and K. Kaibuchi. 2005. CRMP-2 is involved in kinesin-1-dependent transport of the Sra-1/WAVE1 complex and axon formation. *Mol Cell Biol*. 25:9920-35.

Kelly, A.E., H. Kranitz, V. Dotsch, and R.D. Mullins. 2006. Actin binding to the central domain of WASP/Scar proteins plays a critical role in the activation of the Arp2/3 complex. *J Biol Chem*. 281:10589-97.

Kempiak, S.J., H. Yamaguchi, C. Sarmiento, M. Sidani, M. Ghosh, R.J. Eddy, V. Desmarais, M. Way, J. Condeelis, and J.E. Segall. 2005. A neural Wiskott-Aldrich Syndrome protein-mediated pathway for localized activation of actin polymerization that is regulated by cortactin. *J. Biol. Chem.* 280:5836-42.

Kim, A.S., L.T. Kakalis, N. Abdul-Manan, G.A. Liu, and M.K. Rosen. 2000. Autoinhibition and activation mechanisms of the Wiskott-Aldrich syndrome protein. *Nature*. 404:151-8.

Kim, H.J., A.B. DiBernardo, J.A. Sloane, M.N. Rasband, D. Solomon, B. Kosaras, S.P. Kwak, and T.K. Vartanian. 2006a. WAVE1 is required for oligodendrocyte morphogenesis and normal CNS myelination. *J Neurosci*. 26:5849-59.

Kim, Y., J.Y. Sung, I. Ceglia, K.W. Lee, J.H. Ahn, J.M. Halford, A.M. Kim, S.P. Kwak, J.B. Park, S. Ho Ryu, A. Schenck, B. Bardoni, J.D. Scott, A.C. Nairn, and P. Greengard. 2006b. Phosphorylation of WAVE1 regulates actin polymerization and dendritic spine morphology. *Nature*. 442:814-7.

Kitamura, Y., D. Tsuchiya, K. Takata, K. Shibagaki, T. Taniguchi, M.A. Smith, G. Perry, H. Miki, T. Takenawa, and S. Shimohama. 2003. Possible involvement of Wiskott-Aldrich syndrome protein family in aberrant neuronal sprouting in Alzheimer's disease. *Neurosci Lett*. 346:149-52.

Korobova, F., and T. Svitkina. 2008. Arp2/3 Complex Is Important for Filopodia Formation, Growth Cone Motility and Neuritogenesis in Neuronal Cells. *Mol Biol Cell*.

Kreis, P., E. Thevenot, V. Rousseau, B. Boda, D. Muller, and J.V. Barnier. 2007. The p21-activated kinase 3 implicated in mental retardation regulates spine morphogenesis through a Cdc42-dependent pathway. *J Biol Chem*. 282:21497-506.

Krugmann, S., I. Jordens, K. Gevaert, M. Driessens, J. Vandekerckhove, and A. Hall. 2001. Cdc42 induces filopodia by promoting the formation of an IRSp53:Mena complex. *Curr Biol*. 11:1645-55.

Legg, J.A., G. Bompard, J. Dawson, H.L. Morris, N. Andrew, L. Cooper, S.A. Johnston, G. Tramountanis, and L.M. Machesky. 2007. N-wasp involvement in dorsal ruffle formation in mouse embryonic fibroblasts. *Mol Biol Cell*. 18:678-87.

Lewis, A.K., and P.C. Bridgman. 1992. Nerve growth cone lamellipodia contain two populations of actin filaments that differ in organization and polarity. *J Cell Biol*. 119:1219-43.

Li, Z., K. Okamoto, Y. Hayashi, and M. Sheng. 2004. The importance of dendritic mitochondria in the morphogenesis and plasticity of spines and synapses. *Cell*. 119:873-87.

Linder, S., and M. Aepfelbacher. 2003. Podosomes: adhesion hot-spots of invasive cells. *Trends Cell Biol*. 13:376-85.

Lommel, S., S. Benesch, K. Rottner, T. Franz, J. Wehland, and R. Kuhn. 2001. Actin pedestal formation by enteropathogenic Escherichia coli and intracellular motility

of Shigella flexneri are abolished in N-WASP-defective cells. *EMBO Rep*. 2:850-7.

Ma, L., R. Rohatgi, and M.W. Kirschner. 1998. The Arp2/3 complex mediates actin polymerization induced by the small GTP-binding protein Cdc42. *Proc Natl Acad Sci U S A*. 95:15362-7.

Machesky, L.M., S.J. Atkinson, C. Ampe, J. Vandekerckhove, and T.D. Pollard. 1994. Purification of a cortical complex containing two unconventional actins from Acanthamoeba by affinity chromatography on profilin-agarose. *J Cell Biol*. 127:107-15.

Machesky, L.M., and R.H. Insall. 1998. Scar1 and the related Wiskott-Aldrich syndrome protein, WASP, regulate the actin cytoskeleton through the Arp2/3 complex. *Curr Biol*. 8:1347-56.

Machesky, L.M., R.D. Mullins, H.N. Higgs, D.A. Kaiser, L. Blanchoin, R.C. May, M.E. Hall, and T.D. Pollard. 1999. Scar, a WASp-related protein, activates nucleation of actin filaments by the Arp2/3 complex. *Proc. Natl. Acad. Sci. U S A*. 96:3739-44.

Marchand, J.B., D.A. Kaiser, T.D. Pollard, and H.N. Higgs. 2001. Interaction of WASP/Scar proteins with actin and vertebrate Arp2/3 complex. *Nat. Cell Biol.* 3:76-82.

Marrs, G.S., S.H. Green, and M.E. Dailey. 2001. Rapid formation and remodeling of postsynaptic densities in developing dendrites. *Nat. Neurosci.* 4:1006-13.

Matas, O.B., J.A. Martinez-Menarguez, and G. Egea. 2004. Association of Cdc42/N-WASP/Arp2/3 signaling pathway with Golgi membranes. *Traffic*. 5:838-46.

Matus, A. 2000. Actin-based plasticity in dendritic spines. *Science*. 290:754-8.

Matus, A., M. Ackermann, G. Pehling, H.R. Byers, and K. Fujiwara. 1982. High actin concentrations in brain dendritic spines and postsynaptic densities. *Proc. Natl. Acad. Sci. U S A*. 79:7590-4.

McGee, K., M. Zettl, M. Way, and M. Fallman. 2001. A role for N-WASP in invasin-promoted internalisation. *FEBS Lett*. 509:59-65.

McKee, A.C., N.W. Kowall, and K.S. Kosik. 1989. Microtubular reorganization and dendritic growth response in Alzheimer's disease. *Ann Neurol*. 26:652-9.

Merrifield, C.J., B. Qualmann, M.M. Kessels, and W. Almers. 2004. Neural Wiskott Aldrich Syndrome Protein (N-WASP) and the Arp2/3 complex are recruited to sites of clathrin-mediated endocytosis in cultured fibroblasts. *Eur J Cell Biol*. 83:13-8.

Miki, H., K. Miura, and T. Takenawa. 1996. N-WASP, a novel actin-depolymerizing protein, regulates the cortical cytoskeletal rearrangement in a PIP2-dependent manner downstream of tyrosine kinases. *Embo J.* 15:5326-35.

Miki, H., T. Sasaki, Y. Takai, and T. Takenawa. 1998a. Induction of filopodium formation by a WASP-related actin-depolymerizing protein N-WASP. *Nature*. 391:93-6.

Miki, H., S. Suetsugu, and T. Takenawa. 1998b. WAVE, a novel WASP-family protein involved in actin reorganization induced by Rac. *Embo J*. 17:6932-41.

Miki, H., and T. Takenawa. 1998. Direct binding of the verprolin-homology domain in N-WASP to actin is essential for cytoskeletal reorganization. *Biochem Biophys Res Commun*. 243:73-8.

Miki, H., H. Yamaguchi, S. Suetsugu, and T. Takenawa. 2000. IRSp53 is an essential intermediate between Rac and WAVE in the regulation of membrane ruffling. *Nature*. 408:732-5.

Mongiu, A.K., E.L. Weitzke, O.Y. Chaga, and G.G. Borisy. 2007. Kinetic-structural analysis of neuronal growth cone veil motility. *J Cell Sci*. 120:1113-25.

Moreau, V., F. Frischknecht, I. Reckmann, R. Vincentelli, G. Rabut, D. Stewart, and M. Way. 2000. A complex of N-WASP and WIP integrates signalling cascades that lead to actin polymerization. *Nat. Cell Biol.* 2:441-8.

Mullins, R.D., J.A. Heuser, and T.D. Pollard. 1998. The interaction of Arp2/3 complex with actin: nucleation, high affinity pointed end capping, and formation of branching networks of filaments. *Proc. Natl. Acad. Sci. U S A*. 95:6181-6.

Nagase, T., N. Seki, K. Ishikawa, M. Ohira, Y. Kawarabayasi, O. Ohara, A. Tanaka, H. Kotani, N. Miyajima, and N. Nomura. 1996. Prediction of the coding sequences of unidentified human genes. VI. The coding sequences of 80 new genes (KIAA0201-KIAA0280) deduced by analysis of cDNA clones from cell line KG-1 and brain. *DNA Res*. 3:321-9, 341-54.

Newey, S.E., V. Velamoor, E.E. Govek, and L. Van Aelst. 2005. Rho GTPases, dendritic structure, and mental retardation. *J Neurobiol*. 64:58-74.

Nishimura, T., T. Yamaguchi, A. Tokunaga, A. Hara, T. Hamaguchi, K. Kato, A. Iwamatsu, H. Okano, and K. Kaibuchi. 2006. Role of numb in dendritic spine development with a Cdc42 GEF intersectin and EphB2. *Mol Biol Cell*. 17:1273-85.

Node-Langlois, R., D. Muller, and B. Boda. 2006. Sequential implication of the mental retardation proteins ARHGEF6 and PAK3 in spine morphogenesis. *J Cell Sci*. 119:4986-93.

Nozumi, M., H. Nakagawa, H. Miki, T. Takenawa, and S. Miyamoto. 2003. Differential localization of WAVE isoforms in filopodia and lamellipodia of the neuronal growth cone. *J Cell Sci*. 116:239-46.

Ochs, H.D., and A.J. Thrasher. 2006. The Wiskott-Aldrich syndrome. *J Allergy Clin Immunol*. 117:725-38; quiz 739.

Oikawa, T., H. Yamaguchi, T. Itoh, M. Kato, T. Ijuin, D. Yamazaki, S. Suetsugu, and T. Takenawa. 2004. PtdIns(3,4,5)P3 binding is necessary for WAVE2-induced formation of lamellipodia. *Nat Cell Biol*. 6:420-6.

Panchal, S.C., D.A. Kaiser, E. Torres, T.D. Pollard, and M.K. Rosen. 2003. A conserved amphipathic helix in WASP/Scar proteins is essential for activation of Arp2/3 complex. *Nat Struct Biol*. 10:591-8.

Pantaloni, D., R. Boujemaa, D. Didry, P. Gounon, and M.F. Carlier. 2000. The Arp2/3 complex branches filament barbed ends: functional antagonism with capping proteins. *Nat Cell Biol*. 2:385-91.

Papayannopoulos, V., C. Co, K.E. Prehoda, S. Snapper, J. Taunton, and W.A. Lim. 2005. A polybasic motif allows N-WASP to act as a sensor of PIP(2) density. *Mol Cell*. 17:181-91.

Park, E., M. Na, J. Choi, S. Kim, J.R. Lee, J. Yoon, D. Park, M. Sheng, and E. Kim. 2003. The Shank family of postsynaptic density proteins interacts with and promotes synaptic accumulation of the beta PIX guanine nucleotide exchange factor for Rac1 and Cdc42. *J Biol Chem*. 278:19220-9.

Park, S.J., S. Suetsugu, and T. Takenawa. 2005. Interaction of HSP90 to N-WASP leads to activation and protection from proteasome-dependent degradation. *Embo J*. 24:1557-70.

Paunola, E., P.K. Mattila, and P. Lappalainen. 2002. WH2 domain: a small, versatile adapter for actin monomers. *FEBS Lett*. 513:92-7.

Peterson, J.R., L.C. Bickford, D. Morgan, A.S. Kim, O. Ouerfelli, M.W. Kirschner, and M.K. Rosen. 2004. Chemical inhibition of N-WASP by stabilization of a native autoinhibited conformation. *Nat. Struct. Mol. Biol.* 11:747-55.

Pilpel, Y., and M. Segal. 2005. Rapid WAVE dynamics in dendritic spines of cultured hippocampal neurons is mediated by actin polymerization. *J Neurochem*. 95:1401-10.

Pinyol, R., A. Haeckel, A. Ritter, B. Qualmann, and M.M. Kessels. 2007. Regulation of N-WASP and the Arp2/3 complex by Abp1 controls neuronal morphology. *PLoS ONE*. 2:e400.

Pollard, T.D. 2007. Regulation of actin filament assembly by Arp2/3 complex and formins. *Annu Rev Biophys Biomol Struct*. 36:451-77.

Pommereit, D., and F.S. Wouters. 2007. An NGF-induced Exo70-TC10 complex locally antagonises Cdc42-mediated activation of N-WASP to modulate neurite outgrowth. *J Cell Sci*. 120:2694-705.

Portera-Cailliau, C., D.T. Pan, and R. Yuste. 2003. Activity-regulated dynamic behavior of early dendritic protrusions: evidence for different types of dendritic filopodia. *J Neurosci*. 23:7129-42.

Prehoda, K.E., J.A. Scott, R.D. Mullins, and W.A. Lim. 2000. Integration of multiple signals through cooperative regulation of the N-WASP-Arp2/3 complex. *Science*. 290:801-6.

Qualmann, B., and R.B. Kelly. 2000. Syndapin isoforms participate in receptor-mediated endocytosis and actin organization. *J Cell Biol*. 148:1047-62.

Ramesh, N., I.M. Anton, J.H. Hartwig, and R.S. Geha. 1997. WIP, a protein associated with wiskott-aldrich syndrome protein, induces actin polymerization and redistribution in lymphoid cells. *Proc Natl Acad Sci U S A*. 94:14671-6.

Rodal, A.A., O. Sokolova, D.B. Robins, K.M. Daugherty, S. Hippenmeyer, H. Riezman, N. Grigorieff, and B.L. Goode. 2005. Conformational changes in the Arp2/3 complex leading to actin nucleation. *Nat Struct Mol Biol*. 12:26-31.

Rohatgi, R., H.Y. Ho, and M.W. Kirschner. 2000. Mechanism of N-WASP activation by CDC42 and phosphatidylinositol 4, 5-bisphosphate. *J Cell Biol*. 150:1299-310.

Rohatgi, R., L. Ma, H. Miki, M. Lopez, T. Kirchhausen, T. Takenawa, and M.W. Kirschner. 1999. The interaction between N-WASP and the Arp2/3 complex links Cdc42-dependent signals to actin assembly. *Cell*. 97:221-31.

Ryan, T.A., H. Reuter, B. Wendland, F.E. Schweizer, R.W. Tsien, and S.J. Smith. 1993. The kinetics of synaptic vesicle recycling measured at single presynaptic boutons. *Neuron*. 11:713-24.

Saito, T., C.C. Jones, S. Huang, M.P. Czech, and P.F. Pilch. 2007. The interaction of Akt with APPL1 is required for insulin-stimulated Glut4 translocation. *J. Biol. Chem.* 282:32280-7.

Schenck, A., A. Qurashi, P. Carrera, B. Bardoni, C. Diebold, E. Schejter, J.L. Mandel, and A. Giangrande. 2004. WAVE/SCAR, a multifunctional complex coordinating different aspects of neuronal connectivity. *Dev Biol*. 274:260-70.

Scott, E.K., J.E. Reuter, and L. Luo. 2003. Small GTPase Cdc42 is required for multiple aspects of dendritic morphogenesis. *J. Neurosci.* 23:3118-23.

Shekarabi, M., S.W. Moore, N.X. Tritsch, S.J. Morris, J.F. Bouchard, and T.E. Kennedy. 2005. Deleted in colorectal cancer binding netrin-1 mediates cell substrate adhesion and recruits Cdc42, Rac1, Pak1, and N-WASP into an intracellular signaling complex that promotes growth cone expansion. *J Neurosci*. 25:3132-41.

Shen, W., B. Wu, Z. Zhang, Y. Dou, Z.R. Rao, Y.R. Chen, and S. Duan. 2006. Activity-induced rapid synaptic maturation mediated by presynaptic cdc42 signaling. *Neuron*. 50:401-14.

Shin, N., S. Lee, N. Ahn, S.A. Kim, S.G. Ahn, Z. YongPark, and S. Chang. 2007. Sorting nexin 9 interacts with dynamin 1 and N-WASP and coordinates synaptic vesicle endocytosis. *J Biol Chem*. 282:28939-50.

Snapper, S.B., F. Takeshima, I. Anton, C.H. Liu, S.M. Thomas, D. Nguyen, D. Dudley, H. Fraser, D. Purich, M. Lopez-Ilasaca, C. Klein, L. Davidson, R. Bronson, R.C. Mulligan, F. Southwick, R. Geha, M.B. Goldberg, F.S. Rosen, J.H. Hartwig, and F.W. Alt. 2001. N-WASP deficiency reveals distinct pathways for cell surface projections and microbial actin-based motility. *Nat Cell Biol*. 3:897-904.

Soderling, S.H., E.S. Guire, S. Kaech, J. White, F. Zhang, K. Schutz, L.K. Langeberg, G. Banker, J. Raber, and J.D. Scott. 2007. A WAVE-1 and WRP signaling complex regulates spine density, synaptic plasticity, and memory. *J Neurosci*. 27:355-65.

Stamm, L.M., M.A. Pak, J.H. Morisaki, S.B. Snapper, K. Rottner, S. Lommel, and E.J. Brown. 2005. Role of the WASP family proteins for Mycobacterium marinum actin tail formation. *Proc Natl Acad Sci U S A*. 102:14837-42.

Steffen, A., J. Faix, G.P. Resch, J. Linkner, J. Wehland, J.V. Small, K. Rottner, and T.E. Stradal. 2006. Filopodia formation in the absence of functional WAVE- and Arp2/3-complexes. *Mol. Biol. Cell*. 17:2581-91.

Stovold, C.F., T.H. Millard, and L.M. Machesky. 2005. Inclusion of Scar/WAVE3 in a similar complex to Scar/WAVE1 and 2. *BMC Cell Biol*. 6:11.

Strasser, G.A., N.A. Rahim, K.E. VanderWaal, F.B. Gertler, and L.M. Lanier. 2004. Arp2/3 is a negative regulator of growth cone translocation. *Neuron*. 43:81-94.

Sturge, J., J. Hamelin, and G.E. Jones. 2002. N-WASP activation by a beta1-integrin-dependent mechanism supports PI3K-independent chemotaxis stimulated by urokinase-type plasminogen activator. *J Cell Sci*. 115:699-711.

Suetsugu, S., M. Hattori, H. Miki, T. Tezuka, T. Yamamoto, K. Mikoshiba, and T. Takenawa. 2002. Sustained activation of N-WASP through phosphorylation is essential for neurite extension. *Dev Cell*. 3:645-58.

Suetsugu, S., S. Kurisu, T. Oikawa, D. Yamazaki, A. Oda, and T. Takenawa. 2006. Optimization of WAVE2 complex-induced actin polymerization by membrane-bound IRSp53, PIP(3), and Rac. *J Cell Biol*. 173:571-85.

Suetsugu, S., H. Miki, and T. Takenawa. 1998. The essential role of profilin in the assembly of actin for microspike formation. *Embo J*. 17:6516-26.

Suetsugu, S., H. Miki, and T. Takenawa. 1999. Identification of two human WAVE/SCAR homologues as general actin regulatory molecules which associate with the Arp2/3 complex. *Biochem Biophys Res Commun*. 260:296-302.

Suetsugu, S., and T. Takenawa. 2003. Translocation of N-WASP by nuclear localization and export signals into the nucleus modulates expression of HSP90. *J Biol Chem*. 278:42515-23.

Suetsugu, S., T. Tezuka, T. Morimura, M. Hattori, K. Mikoshiba, T. Yamamoto, and T. Takenawa. 2004. Regulation of actin cytoskeleton by mDab1 through N-WASP and ubiquitination of mDab1. *Biochem J*. 384:1-8.

Sung, J.Y., O. Engmann, M.A. Teylan, A.C. Nairn, P. Greengard, and Y. Kim. 2008. WAVE1 controls neuronal activity-induced mitochondrial distribution in dendritic spines. *Proc Natl Acad Sci U S A*.

Suzuki, T., H. Miki, T. Takenawa, and C. Sasakawa. 1998. Neural Wiskott-Aldrich syndrome protein is implicated in the actin-based motility of Shigella flexneri. *Embo J*. 17:2767-76.

Symons, M., J.M. Derry, B. Karlak, S. Jiang, V. Lemahieu, F. McCormick, U. Francke, and A. Abo. 1996. Wiskott-Aldrich syndrome protein, a novel effector for the GTPase CDC42Hs, is implicated in actin polymerization. *Cell*. 84:723-34.

Takenawa, T., and S. Suetsugu. 2007. The WASP-WAVE protein network: connecting the membrane to the cytoskeleton. *Nat. Rev. Mol. Cell Biol.* 8:37-48.

Tashiro, A., A. Minden, and R. Yuste. 2000. Regulation of dendritic spine morphology by the rho family of small GTPases: antagonistic roles of Rac and Rho. *Cereb. Cortex*. 10:927-38.

Torres, E., and M.K. Rosen. 2006. Protein-tyrosine kinase and GTPase signals cooperate to phosphorylate and activate Wiskott-Aldrich syndrome protein (WASP)/neuronal WASP. *J Biol Chem*. 281:3513-20.

Tsuchiya, D., Y. Kitamura, K. Takata, T. Sugisaki, T. Taniguchi, K. Uemura, H. Miki, T. Takenawa, and S. Shimohama. 2006. Developmental expression of neural Wiskott-Aldrich syndrome protein (N-WASP) and WASP family verprolin-homologous protein (WAVE)-related proteins in postnatal rat cerebral cortex and hippocampus. *Neurosci. Res.* 56:459-69.

Udo, H., I. Jin, J.H. Kim, H.L. Li, T. Youn, R.D. Hawkins, E.R. Kandel, and C.H. Bailey. 2005. Serotonin-induced regulation of the actin network for learning-related synaptic growth requires Cdc42, N-WASP, and PAK in Aplysia sensory neurons. *Neuron*. 45:887-901.

Washbourne, P., A. Dityatev, P. Scheiffele, T. Biederer, J.A. Weiner, K.S. Christopherson, and A. El-Husseini. 2004. Cell adhesion molecules in synapse formation. *J Neurosci*. 24:9244-9.

Webb, D.J., H. Zhang, D. Majumdar, and A.F. Horwitz. 2007. alpha5 integrin signaling regulates the formation of spines and synapses in hippocampal neurons. *J Biol Chem*. 282:6929-35.

Welch, M.D., A.H. DePace, S. Verma, A. Iwamatsu, and T.J. Mitchison. 1997a. The human Arp2/3 complex is composed of evolutionarily conserved subunits and is localized to cellular regions of dynamic actin filament assembly. *J Cell Biol*. 138:375-84.

Welch, M.D., A. Iwamatsu, and T.J. Mitchison. 1997b. Actin polymerization is induced by Arp2/3 protein complex at the surface of Listeria monocytogenes. *Nature*. 385:265-9.

Wu, X., Y. Yoo, N.N. Okuhama, P.W. Tucker, G. Liu, and J.L. Guan. 2006. Regulation of RNA-polymerase-II-dependent transcription by N-WASP and its nuclear-binding partners. *Nat Cell Biol*. 8:756-63.

Yamaguchi, H., M. Lorenz, S. Kempiak, C. Sarmiento, S. Coniglio, M. Symons, J. Segall, R. Eddy, H. Miki, T. Takenawa, and J. Condeelis. 2005. Molecular mechanisms of invadopodium formation: the role of the N-WASP-Arp2/3 complex pathway and cofilin. *J. Cell Biol.* 168:441-52.

Yamaguchi, H., H. Miki, S. Suetsugu, L. Ma, M.W. Kirschner, and T. Takenawa. 2000. Two tandem verprolin homology domains are necessary for a strong activation of Arp2/3 complex-induced actin polymerization and induction of microspike formation by N-WASP. *Proc. Natl. Acad. Sci. U S A.* 97:12631-6.

Yamaguchi, H., H. Miki, and T. Takenawa. 2002. Two verprolin homology domains increase the Arp2/3 complex-mediated actin polymerization activities of N-WASP and WAVE1 C-terminal regions. *Biochem Biophys Res Commun*. 297:214-9.

Yarar, D., W. To, A. Abo, and M.D. Welch. 1999. The Wiskott-Aldrich syndrome protein directs actin-based motility by stimulating actin nucleation with the Arp2/3 complex. *Curr. Biol.* 9:555-8.

Zalevsky, J., L. Lempert, H. Kranitz, and R.D. Mullins. 2001. Different WASP family proteins stimulate different Arp2/3 complex-dependent actin-nucleating activities. *Curr Biol*. 11:1903-13.

Zhang, H., and I.G. Macara. 2008. The PAR-6 Polarity Protein Regulates Dendritic Spine Morphogenesis through p190 RhoGAP and the Rho GTPase. *Dev. Cell*. 14:216-26.

Zhang, H., D.J. Webb, H. Asmussen, and A.F. Horwitz. 2003. Synapse formation is regulated by the signaling adaptor GIT1. *J. Cell Biol.* 161:131-42.

Zhang, H., D.J. Webb, H. Asmussen, S. Niu, and A.F. Horwitz. 2005. A GIT1/PIX/Rac/PAK signaling module regulates spine morphogenesis and synapse formation through MLC. *J. Neurosci.* 25:3379-88.

Ziv, N.E., and S.J. Smith. 1996. Evidence for a role of dendritic filopodia in synaptogenesis and spine formation. *Neuron*. 17:91-102.